

Approaches to biological species delimitation based on genetic and spatial dissimilarity

Gabriele d'Angella*, Christian Hennig†

Abstract

The delimitation of biological species, i.e., deciding which individuals belong to the same species and whether and how many different species are represented in a data set, is key to the conservation of biodiversity. Much existing work uses only genetic data for species delimitation, often employing some kind of cluster analysis. This can be misleading, because geographically distant groups of individuals can be genetically quite different even if they belong to the same species. We investigate the problem of testing whether two potentially separated groups of individuals can belong to a single species or not based on genetic and spatial data. Existing methods such as the partial Mantel test and jackknife-based distance-distance regression are considered as well as new approaches, i.e., an adaptation of a mixed effects model, a bootstrap approach, and a jackknife version of partial Mantel. All these methods address the issue that distance data violate the independence assumption for standard inference regarding correlation and regression; a standard linear regression is also considered. The approaches are compared on simulated meta-populations generated with SLiM and GSpace - two software packages that can simulate spatially-explicit genetic data at an individual level. Simulations showed that partial Mantel tests and mixed-effects models have larger power than jackknife-based methods, but tend to display type I error rates slightly above the significance level. An application on brassy ringlets concludes the paper.

1 Introduction

For the delimitation of biological species, empirical data is used to determine “*which groups of individual organisms constitute different populations of a single species and which constitute different species*” (Rannala and Yang, 2020). Species delimitation is crucial to preserve biodiversity and has applications in several areas, such as ecology and medicine (Burbrink and Ruane, 2021). It relies on species conceptualization (De Queiroz, 2007; Hausdorf, 2011). The empirical data employed to delimit species can be molecular (see, e.g., Rannala and Yang (2020) for a review), morphological (Gratton et al., 2016), behavioural (Scapini et al., 2002), ecological (Raxworthy et al., 2007; Rissler and Apodaca, 2007). There are also integrative approaches using different types of data (Edwards and Knowles, 2014) and methods (Carstens et al., 2013).

Also spatial information is key for this task, as witnessed by the increase in publications in the field of landscape genetics (Storfer et al., 2010), which combines population genetics and landscape ecology (Balkenhol et al., 2015). Neglecting geographic information when delimiting species can lead

*Alma Mater Studiorum - University of Bologna, Via Belle Arti, 41 - 40126 Bologna (BO), Italy. E-mail address: gabriele.dangella2@unibo.it

†Alma Mater Studiorum - University of Bologna, Via Belle Arti, 41 - 40126 Bologna (BO), Italy. E-mail address: christian.hennig@unibo.it

to the overestimation of the genetic structure in the data (Frantz et al., 2009). This is more likely to happen in the presence of spatial patterns of genetic differentiation, such as isolation by distance (IBD; Ishida, 2009): clustering methods might wrongly assign individuals to different species given that their genetic dissimilarity increases with geographic separation (Bradburd et al., 2018), violating the assumption of random mating within the population (panmixia).

A way to include spatial information in molecular species delimitation routines is to study the relationship between genetic dissimilarities and geographic distance. The investigation of this relationship has a long tradition in the population genetics literature, where it was pursued to study migration models (Kimura and Weiss, 1964) or estimate demographic parameters (Slatkin, 1993; Rousset, 1997; Clarke et al., 2002). While isolation by distance assumes that the genetic dissimilarity between two individuals simply increases with the Euclidean distance (or, if we deal with latitude and longitude, the great-circle distance, i.e., the shortest distance between two locations on the surface of a sphere), isolation by resistance (IBR; McRae, 2006) takes into account landscape features such as rivers and heights: this translates in developments like the least-cost path approach (Adriaensen et al., 2003), the circuit-based framework (McRae et al., 2008) or the least-cost transect analysis (Van Strien et al., 2012), in which a more sophisticated “landscape” dissimilarity measure replaces the Euclidean distance in the attempt to explain genetic dissimilarities between individuals. In this perspective, IBR or isolation by environment (Wang and Bradburd, 2014) models are tested against the IBD model, which is seen as a null or baseline model (MacDonald et al., 2020). We will work with the Euclidean distance as geographical dissimilarity here, but all the considered methods will also work with other geographic dissimilarities.

Consider a setup with two putative groups of individuals to be tested for conspecificity. Inference is based on checking whether the relationship between genetic and geographic dissimilarity differs between pairs of individuals in the same group and pairs in different groups (see Sections 2 and 5 for details). Each of the three panels in Figure 1 shows genetic and geographic dissimilarities of two groups for which a test for conspecificity is of interest. Distances within the two groups are black circles and red triangles, distances between the groups are green diamonds. The plots show some (albeit weak) tendency that larger genetic distance comes with larger geographic distance, also within groups. On the left side, genetic (“shared allele”) distances between groups seem slightly higher on average than genetic distances within groups, but also the geographic distances tend to be higher, and just from looking at the data it is not clear cut whether larger genetic distances between groups can be explained by the geographic distances only (in which case there is no reason to consider the two groups as different species), even less so in the middle. On the right side, it is clear that genetic distances between groups are much larger than they could be expected to be in case the two groups belonged to the same species.

The impact of grouping on the genetic dissimilarity can be quantified controlling for the effect of geographic distance. Medrano et al. (2014) used a permutation-based partial Mantel test (PMT; Smouse et al., 1986) to assess the significance of the partial correlation coefficient between genetic and grouping dissimilarities given the geographic distance, where the grouping dissimilarity is defined as 0 if a pair of individuals is in the same group and 1 otherwise. Hausdorf and Hennig (2020) suggested to jackknife test for whether a regression fitted on the within-group distances can also explain the between-groups distances. Clarke et al. (2002) employed individual random effects in order to model the dependence between dissimilarities belonging to the same individual. This approach can be extended and adapted to the IBD problem by testing for an effect of the grouping dissimilarity as we do in the present paper. Also, we investigate partial Mantel tests using jackknife or bootstrap instead of permutations. All these techniques take into account the dependence between dissimilarities involving the same individual. For exploring how much of a difference taking into account the dependence between dissimilarities actually makes, we also consider a multiple regression

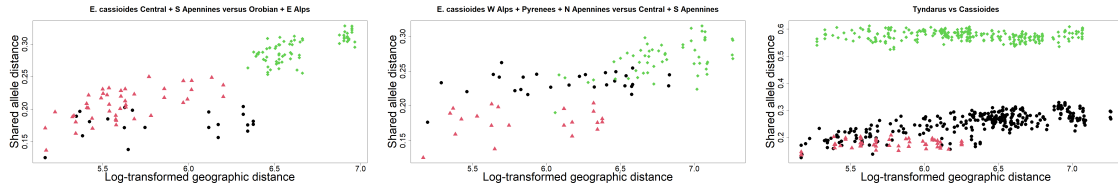


Figure 1: Log-transformed geographic distances vs. Shared allele distances for three pairs of groups from the brassy ringlets data (left side *E. Cassioides central + S. Apennines* vs. *Orobian + E. Alps*; middle *E. Cassioides W. Alps, Pyrenees + N. Apennines* vs. *central + S. Apennines*; right side *E. Tyndarus* vs. *E. Cassioides*), see Section 5, for which conspecificity is of interest. The black circles (first group) and red triangles (second group) show distances between pairs of individuals belonging to the same group. The green diamonds show the distances between two individuals belonging to different groups.

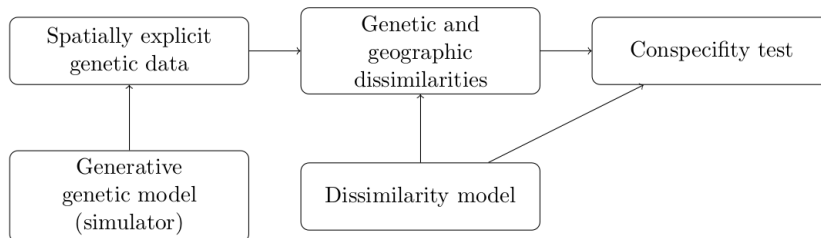


Figure 2: The conspecificity tests treated here are computed on genetic and geographic dissimilarities assuming models for general dissimilarities (i.e., not taking into account how exactly the dissimilarities came about). The dissimilarities are computed from the originally observed spatially explicit genetic data, which in our simulation study are simulated from generative genetic models.

with genetic dissimilarities as response and geographic and grouping dissimilarities as explanatory variables. A similar model was used by Spriggs et al. (2018) to integrate a rich molecular species delimitation analysis.

There exists only anecdotal evidence of the performance of the methods in Medrano et al. (2014), Spriggs et al. (2018) and Hausdorf and Hennig (2020), and they have not been systematically assessed from a statistical perspective. The study presented here consists in a systematic comparison of the type I error rate and power of the aforementioned methods based on simulating spatially-explicit genetic data sets generated by the simulators GSpace (Virgoulay et al., 2021b) and SLiM (Haller and Messer, 2023).

A distinctive feature of the present study is that the genetic dissimilarities on which inference is based are much simpler than the data from which they are computed, see Section 2. To our knowledge, due to complexity, currently no tests for conspecificity exist that operate directly on the genetic information and take into account geographic distance. GSpace and SLiM provide sophisticated models for the genetic data, but the inference does not use such models. Instead it is based on much simpler models for the dissimilarities without taking into account how these were computed from the original genetic data, see Figure 2. Here we confront such inference with the more complex genetic models for exploring its statistical characteristics. Methods and results may be relevant also for other problems where regression between dissimilarities is of interest.

Given that the species concept in biology is somewhat controversial and there is biological differentiation between populations at different levels (there are species that are more or less closely related, and there is differentiation also below the species level; see, e.g., De Queiroz (2007)), any result of the treated tests should not be taken as conclusive regarding conspecificity. The aim is just to formalise a key aspect of the information in the data.

This paper is organized as follows: the data and distances are introduced in section 2, then all methods are discussed in section 3. The two simulators used in this study and the results obtained with them are discussed in section 4. Section 5 presents an application to the brassy ringlets data examined by Gratton et al. (2016). Section 6 concludes the paper.

2 Data and dissimilarities

Spatially explicit genetic data consists of individuals carrying information about their location and genetic make-up. Methods will be applied on individuals from two groups, with known membership. Hence, two columns will correspond to the unit’s coordinates (northings and eastings, latitude and longitude, etc.), one column will report the group labels (either group 1 or 2) and the other P columns will be loci (locations on the DNA). Individual-level codominant data, such as SNPs or microsatellites, with diploid genotypes will be considered (Balkenhol et al., 2015, ch. 3): this means that each locus will contain two alleles. Following (Hausdorf and Hennig, 2019) we represent alleles by single characters although elsewhere in the literature more elaborate coding is used (Rousset, 2008). The resulting $n \times (P + 3)$ data frame will be denoted by

$$\mathbf{Z} = \begin{pmatrix} \mathbf{z}_1 \\ \vdots \\ \mathbf{z}_n \end{pmatrix} = \begin{pmatrix} z_1^x & z_1^y & z_1^c & Z_1^1 & \cdots & Z_1^P \\ z_2^x & z_2^y & z_2^c & Z_2^1 & \cdots & Z_2^P \\ \vdots & \vdots & \vdots & \ddots & \vdots & \vdots \\ z_n^x & z_n^y & z_n^c & Z_n^1 & \cdots & Z_n^P \end{pmatrix},$$

where each observed locus Z_i^p , $p = 1, \dots, P$, is a set of characters, like $\{A, B\}$ for heterozygous loci (“BA”) or $\{B\}$ for homozygous ones (“BB”); also note that alleles are arranged in lexicographical order in the sets because a meaningful order is not normally observable. Each \mathbf{z}_i is a $1 \times (P + 3)$ vector representing the i^{th} individual.

In this study, the Euclidean distance will be employed as geographic distance (subscript x):

$$d_x(\mathbf{z}_i, \mathbf{z}_j) = \sqrt{(z_i^x - z_j^x)^2 + (z_i^y - z_j^y)^2}.$$

As genetic dissimilarity (subscript y), the **shared allele dissimilarity** (Bowcock et al., 1994) will be used:

$$d_y(\mathbf{z}_i, \mathbf{z}_j) = 1 - \frac{1}{2P} \sum_{p=1}^P |Z_i^p \cap Z_j^p| \cdot [1 + \mathbb{1}(|Z_i^p| + |Z_j^p| = 2)], \quad (2.1)$$

where $\mathbb{1}(\text{condition}) = 1$ if the condition is true and zero otherwise. In real data occasionally there is missing data (missing loci). In this case d_y just averages over the loci that are non-missing in both \mathbf{z}_i and \mathbf{z}_j . If there are no missing values, the shared allele dissimilarity is actually a distance, but missing values can cause a violation of the triangle inequality.

It is easy to see that, the larger P , the finer is the quantification of the genetic dissimilarity between two species, as more sites are available for the comparison of two individuals’ genetic information.

Let $n_j = |\{i : z_i^c = j\}|$ be the number of individuals belonging to group $j = 1, 2$. These represent the two candidate (or putative) species to be tested for conspecificity. In practice, this grouping information can be based on morphological, behavioural or even spatial grounds or can simply represent the researcher's hypothesis. The number of geographic distances in the dataset amounts to:

$$\frac{1}{2}(n_1 + n_2)(n_1 + n_2 - 1) = \underbrace{\frac{1}{2}n_1(n_1 - 1)}_{\text{within group 1}} + \underbrace{\frac{1}{2}n_2(n_2 - 1)}_{\text{within group 2}} + \underbrace{n_1n_2}_{\text{between groups}},$$

to be stored in the following $n \times n$ block matrix, with $n = n_1 + n_2$,

$$\mathbf{D}_x = \left(\begin{array}{c|c} \mathbf{D}_x^{11} & \mathbf{D}_x^{12} \\ \hline \mathbf{D}_x^{21} & \mathbf{D}_x^{22} \end{array} \right) = \left(\begin{array}{cccc|cccc} 0 & d_x(\mathbf{z}_1, \mathbf{z}_2) & \cdots & d_x(\mathbf{z}_1, \mathbf{z}_{n_1}) & d_x(\mathbf{z}_1, \mathbf{z}_{n_1+1}) & \cdots & d_x(\mathbf{z}_1, \mathbf{z}_{n_1+n_2}) \\ d_x(\mathbf{z}_2, \mathbf{z}_1) & 0 & \cdots & d_x(\mathbf{z}_2, \mathbf{z}_{n_1}) & d_x(\mathbf{z}_2, \mathbf{z}_{n_1+1}) & \cdots & d_x(\mathbf{z}_2, \mathbf{z}_{n_1+n_2}) \\ \vdots & \vdots & \ddots & \vdots & \vdots & \ddots & \vdots \\ d_x(\mathbf{z}_{n_1}, \mathbf{z}_1) & d_x(\mathbf{z}_{n_1}, \mathbf{z}_2) & \cdots & 0 & d_x(\mathbf{z}_{n_1}, \mathbf{z}_{n_1+1}) & \cdots & d_x(\mathbf{z}_{n_1}, \mathbf{z}_{n_1+n_2}) \\ \hline d_x(\mathbf{z}_{n_1+1}, \mathbf{z}_1) & d_x(\mathbf{z}_{n_1+1}, \mathbf{z}_2) & \cdots & d_x(\mathbf{z}_{n_1+1}, \mathbf{z}_{n_1}) & 0 & \cdots & d_x(\mathbf{z}_{n_1+1}, \mathbf{z}_{n_1+n_2}) \\ \vdots & \vdots & \ddots & \vdots & \vdots & \ddots & \vdots \\ d_x(\mathbf{z}_{n_1+n_2}, \mathbf{z}_1) & d_x(\mathbf{z}_{n_1+n_2}, \mathbf{z}_2) & \cdots & d_x(\mathbf{z}_{n_1+n_2}, \mathbf{z}_{n_1}) & d_x(\mathbf{z}_{n_1+n_2}, \mathbf{z}_{n_1+1}) & \cdots & 0 \end{array} \right),$$

where matrix \mathbf{D}_x^{11} stores the distances among the observations belonging to group 1, \mathbf{D}_x^{22} those within group 2 and $\mathbf{D}_x^{12} = (\mathbf{D}_x^{21})^\top$ those among individuals of different groups. \mathbf{D}_x carries redundant information: it is sufficient to work with the lower triangular matrix $\{d_x(\mathbf{z}_r, \mathbf{z}_c)\}_{r>c}$. Analogously, the $n \times n$ block matrices \mathbf{D}_y and \mathbf{D}_g store the genetic and grouping dissimilarities.

We will later use the sets of all index pairs referring to within-group and between-group dissimilarities, respectively:

$$W = \{r, c \leq n \mid c < r \leq n_1 \vee n_1 < c < r\}, \quad B = \{r, c \leq n \mid r > n_1 \wedge c \leq n_1\}.$$

In order to improve the linearity between geographic and genetic dissimilarities, it is often advantageous to use log-transformed geographic distances as is done for example in Vekemans and Hardy (2004), Rousset (1997), and Hausdorf and Hennig (2020). Zero geographical distances can occur if two individuals are observed in the same location. Therefore, following Hausdorf and Hennig (2020), the following transformation is considered:

$$f(d_x(\mathbf{z}_r, \mathbf{z}_c)) = \ln(d_x(\mathbf{z}_r, \mathbf{z}_c) + F_x^{-1}(0.25)), \quad (2.2)$$

where

$$F_x^{-1}(q) = \inf\{d : F_x(d) \geq q\}, \quad \text{with} \\ F_x(d) = \frac{1}{w} \sum_{c < r \leq n} \mathbb{1}(d_x(\mathbf{z}_r, \mathbf{z}_c) \leq d)$$

being the empirical cdf of all geographic distances in the dataset, and $w = n(n-1)/2$. In our comparative study we will consider both untransformed and log-transformed \mathbf{D}_x . In order to keep notation light, all methods will be described using untransformed geographic distances.

Although the shared allele distance is used here, the discussed methods are based on models for dissimilarities that do not rely on the specific dissimilarity. The methods can therefore also be applied to other dissimilarities. In conspecificity testing, sometimes data come at population level with genetic distances between populations rather than individuals, e.g., in Clarke et al. (2002) and one example in Hausdorf and Hennig (2020).

3 Methods

The methodologies presented here leverage the information on the relationship between the distances in \mathbf{D}_y and \mathbf{D}_x with the aim of confirming or falsifying a conspecificity presumption encoded in \mathbf{D}_g . In the presence of isolation by distance behaviour (positive association between genetic and geographic dissimilarities), two groups of individuals belonging to the same species might display a certain degree of genetic structure that is explained by their geographic separation. If the genetic dissimilarities are too large to be compatible with the geographic separation between the two groups, this will constitute evidence for lineage separation, i.e., for distinctness. As Hausdorf and Hennig (2020) write, “*it is often difficult to assess whether observed differences between allopatric meta-populations would be sufficient to prevent the fusion of these meta-populations upon contact.*” In these situations, non-spatial models (to whom the putative grouping is often ascribed in practical applications) may be biased and IBD patterns should be taken into account (Meirmans, 2012).

The computation of dissimilarities implies information loss: the complex biological mechanisms (e.g., dispersal, see Cayuela et al., 2018) that act on the allele frequencies of the two investigated putative species have an indirect effect on the relationship between genetic and geographic dissimilarities, which can be non-linear (Hutchison and Templeton, 1999). The methods discussed here do not attempt to model such evolutionary processes, but rather work at the dissimilarity level, where the information from the P loci is summarized. The conspecificity null hypothesis is operationalised by these methods as having the same trend in the relation between genetic and geographic dissimilarities within groups and between groups. For the alternative hypothesis, genetic dissimilarities would be expected to be larger between groups than within groups when adjusted for geographic distances. The methods are based on linear regression and correlation, i.e., they assume linearity. Note however that it can normally be expected with enough data that a zero correlation or regression slope can also be rejected if the relation is nonlinear but monotonic. Therefore the methods can be used also to detect nonlinear monotonic deviations from the null hypothesis (Székely et al. (2007) even show that for Euclidean data independence is equivalent to a “distance correlation”, closely related to what is considered here being zero). Furthermore, the methods treated here do not require the triangle inequality, and monotonic transformations of dissimilarities can also be used.

In the following, the statistical methods involved in this comparative study are described.

3.1 Regression on dissimilarities with jackknife testing

Hausdorf and Hennig (2020) proposed to regress the genetic dissimilarities on the log-transformed geographic distances trying to clarify whether the genetic structure found between the two candidate species can be compatible with their IBD behaviour. To this end, a regression line based on the within-group dissimilarities (red and black observations in Figure 1) is compared with a regression line based on all dissimilarities. The null hypothesis of conspecificity is rejected if the between-groups dissimilarities (green in Figure 1) are systematically too large compared to what would be expected from the regression computed on the within-group dissimilarities. Dependence between dissimilarities is taken into account by running the test using a jackknife scheme that treats the individuals rather than the dissimilarities as observational units.

This approach is complicated by the fact that the test just mentioned relies on a single regression line being appropriate for the within-group dissimilarities in both groups. Hausdorf and Hennig (2020) propose a test protocol where it is first tested whether this is the case (H_{01}). Then, depending on the result, either a null hypothesis of a joint regression for all dissimilarities is tested (H_{02} , corresponding to conspecificity), or, in case that H_{01} is rejected, it is tested whether the between-group distances are in line with at least one of the group-wise regressions of the within-group

dissimilarities (H_{03} ; in case that this is rejected, it is taken as evidence against conspecificity, whereas non-rejection is an ambiguous result that would need closer biological investigation).

The first of the three tests focuses on the relationship between genetic and geographic dissimilarities within the two groups, assuming the following linear relationship:

$$d_y(\mathbf{z}_r, \mathbf{z}_c) = \begin{cases} a_1 + b_1 \{d_x(\mathbf{z}_r, \mathbf{z}_c) - \bar{d}_x^W\} + e(\mathbf{z}_r, \mathbf{z}_c) & \text{with } c < r \leq n_1 \\ a_2 + b_2 \{d_x(\mathbf{z}_r, \mathbf{z}_c) - \bar{d}_x^W\} + e(\mathbf{z}_r, \mathbf{z}_c) & \text{with } n_1 < c < r \end{cases}. \quad (3.1)$$

a_1 , b_1 , a_2 and b_2 are estimated via least squares, and

$$\bar{d}_x^W = \frac{1}{|W|} \sum_{r,c \in W} d_x(\mathbf{z}_r, \mathbf{z}_c)$$

is the mean within-group geographic distance taken over both candidate species. The errors e in (3.1) are assumed to have zero mean, but not to be independent. Only the genetic random variation of individuals is assumed to be independent, but not dissimilarities involving the same individual.

The first test tests $H_{01} : a_1 = a_2$ and $b_1 = b_2$. It is tested against the two-sided alternative that $a_1 - a_2 \neq 0$ or $b_1 - b_2 \neq 0$. Both of these are tested and combined using Bonferroni, i.e., multiplying the minimum of the two p-values by 2.

In order to deal with the dependence between dissimilarities, Hausdorf and Hennig (2020) use non-parametric jackknife (already suggested by Clarke et al. (2002)) to obtain a measure of the variability of the estimates. Jackknifing (Efron and Tibshirani, 1993, ch. 11) here consists in computing as many OLS estimates as the number of individuals involved in a given regression model (e.g., n_1 for group 1) by fitting it on the n_1 datasets obtained by removing one individual at a time. In this particular setup, the removal of one individual implies the removal of all the dissimilarities related to it, so each jackknife replicate of the OLS estimates for group 1 is based on $(n_1 - 1)(n_1 - 2)/2$ data points instead of $n_1(n_1 - 1)/2$.

In jackknifing, so-called pseudovalues u_i , $1 = 1, \dots, n$ for a statistic U computed on data \mathbf{X} with n observations are computed as $u_i = nU(\mathbf{X}) - (n - 1)U(\mathbf{X}_{(i)})$ where $\mathbf{X}_{(i)}$ has the i th observation left out. The variability of the difference between parameter estimates is quantified by pooling the within-group jackknife estimates of standard error (Efron and Tibshirani, 1993, ch. 11) in order to run a Welch's t-test (Welch, 1947).

This principle is applied here to both the difference between intercepts and to the difference between slopes of the two within-group regressions, where the null hypothesis for Welch's t-test is that the expected difference is zero, see Hausdorf and Hennig (2020) for more details. Jackknife testing is a heuristic idea that has a theoretical justification in specific situations, of which the assumptions are not fulfilled here. Therefore, its characteristics have to be explored experimentally in all but the simplest situations, which is done here in Section 4.

If H_{01} is not rejected, a unique regression is fitted on all the within-group dissimilarities, regardless of the membership, because the IBD behaviour of the two candidate species looks compatible. In this situation, hypothesis H_{02} is tested. The following ordinary least squares model is fitted:

$$d_y(\mathbf{z}_r, \mathbf{z}_c) = a_* + b_*(d_x(\mathbf{z}_r, \mathbf{z}_c) - \bar{d}_x^W) + e(\mathbf{z}_r, \mathbf{z}_c) \quad (3.2)$$

where $\mathbb{E}(e(\mathbf{z}_r, \mathbf{z}_c)) = 0$ and $r, c \in W$. This fit will be compared with the following model, which is based on all the dissimilarities in the dataset (within and between-group), regardless of the grouping:

$$d_y(\mathbf{z}_r, \mathbf{z}_c) = a + b(d_y(\mathbf{z}_r, \mathbf{z}_c) - \bar{d}_x^W) + e(\mathbf{z}_r, \mathbf{z}_c) \quad (3.3)$$

where $c < r \leq n$ and $\mathbb{E}(e(\mathbf{z}_r, \mathbf{z}_c)) = 0$. Define $\bar{d}_x^B = \frac{1}{|B|} \sum_{r,c \in B} d_x(\mathbf{z}_r, \mathbf{z}_c)$, the average between-group geographical distance. $H_{02} : a = a^*$ and $b = b^*$ is then tested against the one-sided alternative

$$a + b(\bar{d}_x^B - \bar{d}_x^W) > a_* + b_*(\bar{d}_x^B - \bar{d}_x^W), \quad (3.4)$$

i.e., genetic dissimilarities predicted at \bar{d}_x^B by all dissimilarities combined are systematically larger than predicted by within-group dissimilarities only. The statistic on which jackknife testing is based is

$$\hat{a} + \hat{b}(\bar{d}_x^B - \bar{d}_x^W) - \hat{a}_* - \hat{b}_*(\bar{d}_x^B - \bar{d}_x^W), \quad (3.5)$$

where \hat{a} , \hat{b} , \hat{a}_* and \hat{b}_* are the corresponding OLS estimates.

If H_{01} is rejected, the IBD behaviour of the two candidate species cannot be described by a unique model and model (3.1) is adopted. In this situation, H_{03} is tested, that is, the compatibility of IBD behaviour and genetic structure is checked for each group separately. Two models similar to (3.3) are set up, each one comprising within-group dissimilarities from one of the groups only, together with the between-group dissimilarities, and two jackknife tests are run on statistics analogous to (3.5). $H_{03} : a_j = a_j^*$ and $b_j = b_j^*$ for at least one of $j = 1, 2$ is tested, where a_j, b_j refer to regressions based on dissimilarities within group j only, and a_j^*, b_j^* refer to regressions based on all dissimilarities involving a member of group j . The alternative is defined by analogy to (3.4). The test rejects H_{03} if the maximum of the p-values for the two tests regarding groups $j = 1, 2$ is too small. Note that jackknifing these tests involves two different kinds of pseudovalues. For example consider the test regarding group 1. Members of group 1 are involved in dissimilarities between other members of group 1 and group 2, whereas members of group 2 are only involved in dissimilarities to members of group 1. This is accounted for by the computation of the jackknife estimate of the standard error to be used for the t-test, see Hausdorf and Hennig (2020) and the documentation of the `prabclus` R-implementation (Hausdorf and Hennig, 2019) for details.

A rejection to the test for either H_{02} or H_{03} constitutes evidence against the null hypothesis of conspecificity, suggesting that the relationship between genetic and geographic dissimilarities displayed by the two meta-populations cannot explain their genetic differences and they might thus represent two separated lineages.

3.2 The partial Mantel test

The null hypothesis of the simple Mantel test states that “the distances among objects in matrix \mathbf{D}_y are not (linearly or monotonically) related to the corresponding distances in \mathbf{D}_x ” (Legendre and Legendre, 2012, p. 600). The original test statistic by Mantel (1967) was a cross-product of the vectors of dissimilarities,

$$\sum_{c < r \leq n} d_y(\mathbf{z}_r, \mathbf{z}_c) \cdot d_x(\mathbf{z}_r, \mathbf{z}_c),$$

the standardized version of which corresponds to the sample correlation coefficient between the vectors of dissimilarities:

$$r(\mathbf{D}_y, \mathbf{D}_x) = \frac{\sum_{c < r \leq n} (d_y(\mathbf{z}_r, \mathbf{z}_c) - \bar{d}_y)(d_x(\mathbf{z}_r, \mathbf{z}_c) - \bar{d}_x)}{\sqrt{\sum_{c < r \leq n} (d_y(\mathbf{z}_r, \mathbf{z}_c) - \bar{d}_y)^2 \sum_{c < r \leq n} (d_x(\mathbf{z}_r, \mathbf{z}_c) - \bar{d}_x)^2}}, \quad (3.6)$$

where $\bar{d}_y = \frac{1}{w} \sum_{c < r \leq n} d_y(\mathbf{z}_r, \mathbf{z}_c)$ is the overall average genetic dissimilarity and $\bar{d}_x = \frac{1}{w} \sum_{c < r \leq n} d_x(\mathbf{z}_r, \mathbf{z}_c)$ is the overall average geographic distance.

Partial Mantel tests were proposed by Smouse et al. (1986) and are based on a partial correlation coefficient here defined as

$$r(\mathbf{D}_y, \mathbf{D}_g | \mathbf{D}_x) = \frac{r(\mathbf{D}_y, \mathbf{D}_g) - r(\mathbf{D}_y, \mathbf{D}_x)r(\mathbf{D}_g, \mathbf{D}_x)}{\sqrt{(1 - r(\mathbf{D}_y, \mathbf{D}_x)^2)(1 - r(\mathbf{D}_g, \mathbf{D}_x)^2)}}. \quad (3.7)$$

(3.7) quantifies the correlation between the genetic dissimilarities and the grouping distances after having accounted for the geographic distances. Medrano et al. (2014) tested the null hypothesis that this partial correlation was equal to zero in order to ascribe the genetic structure found in two subgroups of trumpet daffodils to their lineage separation. The rejection of such hypothesis led them to maintain that the IBD behaviour displayed by the groups was not sufficient to explain the genetic dissimilarity found between the groups and that these should therefore not be considered conspecific. In Figure 1 the null hypothesis means that conditionally on geographic distances between-groups genetic dissimilarities (i.e., green) are not systematically larger or smaller than within-group ones (i.e., red or black).

Hypothesis testing is usually carried out by means of permutations, although there exists an asymptotically normal transformation of (3.6) (Legendre and Legendre, 2012, p. 600). Legendre (2000) carried out empirical comparisons of four permutation strategies for partial Mantel tests. His first strategy, the one used in this study, consists in permuting just one of the three dissimilarity matrices and recomputing the partial correlation coefficient a large number of times. The default number of permutations in the `ecodist` package by Goslee and Urban (2007), which was used in this study, is 1000. For each of these 1000 iterations, rows and corresponding columns in matrix \mathbf{D}_y are permuted to yield \mathbf{D}_y^* , which implies the modification of $r(\mathbf{D}_y^*, \mathbf{D}_g)$ and $r(\mathbf{D}_y^*, \mathbf{D}_x)$ to be included in (3.7). If the two groups are separated species, the partial correlation between genetic and group dissimilarities should be positive (larger genetic dissimilarity between groups). Therefore a one-sided test is carried out, and the associated p -value is equal to the share of $r(\mathbf{D}_y^*, \mathbf{D}_g | \mathbf{D}_x)$ permutation replicates that are at least as large as the original value $r(\mathbf{D}_y, \mathbf{D}_g | \mathbf{D}_x)$. Legendre (2000) remarked that this permutation strategy may lead to inflated type-I error if outlying dissimilarity values are present in the data, whereas skewness in the dissimilarities distribution should not represent an issue.

Testing with jackknife Significance in partial Mantel tests is typically assessed via permutations. According to Hausdorf and Hennig (2020), this might introduce a distortion when the within-group geographic dissimilarities tend to be small with respect to the between-groups ones, which is often the case. By systematically altering the distribution of geographic distances within the groups, the permutation strategy might have a strong effect on the estimation of the partial correlation coefficient.

A possible way to prevent this potential distortion is to jackknife the partial correlation (3.7), leaving one individual out at a time, and then generate pseudovalues and run a t-test as explained in Section 3.1.

Testing with bootstrap Another option to assess the variability of the partial correlation coefficient $r(\mathbf{D}_y, \mathbf{D}_g | \mathbf{D}_x)$ is by resampling n individuals with replacement, generating nonparametric bootstrap samples. This idea was discouraged in Clarke et al. (2002) and Hausdorf and Hennig (2020) because, whenever two identical individuals are sampled more than once, the associated dissimilarities will be equal to zero, generating bootstrap samples that in most cases tend to display a larger proportion of zero dissimilarities with respect to the original data. However, to date, no systematic study has demonstrated the performance of nonparametric bootstrap for species delimitation tasks.

A seminal reference for this technique is Efron and Tibshirani (1993). We use the *bias-corrected* (BC) bootstrap confidence intervals here, defined and motivated in Efron and Tibshirani (1993, ch. 22.5). The null hypothesis of conspecificity is rejected in the lower bound of a $(1 - 2\alpha)$ bootstrap confidence interval (α -quantile of the bootstrap distribution adjusted for bias correction) for the partial correlation (3.7) is larger than 0.

3.3 The linear mixed effects model

Another approach to model the dependence between dissimilarities involving the same individual is via introducing individual random effects into a regression between geographic and genetic dissimilarities.

Clarke et al. (2002) proposed such a model. They were working with population-level genetic and geographic data. After centering the geographic distances to remove correlation between the intercept and slope estimates, they extended the linear regression between genetic and (log-transformed) geographic distances by introducing one random effect for each of the two populations on which the dissimilarity value was based. With the notation defined above, it is possible to specify their model as

$$d_y(\mathbf{z}_r, \mathbf{z}_c) = a + b(d_x(\mathbf{z}_r, \mathbf{z}_c) - \bar{d}_x) + \tau_r + \tau_c + \epsilon(\mathbf{z}_r, \mathbf{z}_c) \quad \text{with } n \geq r > c, \quad (3.8)$$

where a is a constant term, τ_r is a random effect representing the average deviation of d_y values involving population r from that expected from its d_x distances to the other populations and τ_r and $\epsilon(\mathbf{z}_r, \mathbf{z}_c)$ are assumed to be independent with $\epsilon(\mathbf{z}_r, \mathbf{z}_c)$ i.i.d. normally distributed. This specification assumes that dependence between two dissimilarities involving the same population can be expressed by an additive random value. Technically this allows for dissimilarities smaller than zero, and does not take into account dependence that involves more than two pairs of populations, as exists for distances at least due to the triangle inequality. The model can therefore not be fully correct for a regression between distances, but given that all models are idealisations and simplifications, the model can still be suitable if it allows for inference with good performance characteristics.

The authors fitted the model via restricted maximum likelihood (REML). It has gained popularity in the landscape genetics literature (Peterman and Pope, 2021), being used to assess the effect of landscape variables on gene flow (Van Strien et al., 2012) and for landscape model selection (Shirk et al., 2018). It can be fitted using the `mlpe_rga` function from the `ResistanceGA` R package (Peterman, 2018), based on the `lme4` package (Bates et al., 2015).

In order to apply model (3.8) for species delimitation, a fixed effect associated with the grouping distance \mathbf{D}_g needs to be incorporated:

$$d_y(\mathbf{z}_r, \mathbf{z}_c) = b_0 + b_1 d_x(\mathbf{z}_r, \mathbf{z}_c) + b_2 d_g(\mathbf{z}_r, \mathbf{z}_c) + \tau_r + \tau_c + \epsilon(\mathbf{z}_r, \mathbf{z}_c) \quad \text{with } n \geq r > c. \quad (3.9)$$

b_2 here is an intercept update for between group genetic dissimilarities, and the null hypothesis $b_2 = 0$ corresponds to conspecificity, which is tested against the one-sided alternative $b_2 > 0$. In Figure 1 b_2 would be the amount by which the green between-groups dissimilarities are on average higher than the red and black within-group dissimilarities. This is similar to H_{02} in Section 3.1, assuming implicitly that there is no difference between the within-group regressions for group 1 and group 2. Even if there is such a difference, it can be seen as relevant to whether the dissimilarities between groups are systematically larger than a model defined on the aggregated within-group dissimilarities.

Note that different from the approaches in Sections 3.1 and 3.2, (3.9) provides a *generative* model for dissimilarities, but we will not use it as such because it does not use information about the underlying genetic dissimilarities, and also, as argued above, it cannot be fully correct for these.

The test can be based on profile likelihood-based confidence intervals (CI) (Venzon and Moolgavkar, 1988; Royston, 2007). The null hypothesis is rejected if the lower boundary of the $(1 - 2\alpha)$

profile likelihood-based CI is larger than zero. These CIs are obtained in R via the `confint` function applied on the `mlpe_rga` output. Profile-likelihood-based CIs are connected to likelihood ratio tests. Therefore, model (3.9) should not be fitted with REML (West et al., 2022).

A related approach was used by Yang (2004) for “*estimating and testing for isolation by distance*”. Instead of introducing random effects explicitly, several standard correlation patterns for the $\epsilon(\mathbf{z}_r, \mathbf{z}_c)$ as available in the SAS PROC MIXED (SAS Institute, 2001) were used to model the dependence in the dissimilarities. This can be expected to be inferior to (3.9), because it does not use the information which dissimilarities belong to the same individual.

A linear regression model ignoring dependence In our study we will also compare a straight linear regression model without the random effects that ignores the dependence between dissimilarities:

$$d_y(\mathbf{z}_r, \mathbf{z}_c) = b_0^* + b_1^* d_x(\mathbf{z}_r, \mathbf{z}_c) + b_2^* d_g(\mathbf{z}_r, \mathbf{z}_c) + \epsilon(\mathbf{z}_r, \mathbf{z}_c) \quad \text{with } n \geq r > c, \quad (3.10)$$

assuming $\epsilon(\mathbf{z}_r, \mathbf{z}_c)$ i.i.d. normally distributed with zero mean. The null hypothesis is once more $b_2^* = 0$, tested against $b_2^* > 0$ with the standard regression t-test. A similar approach has been taken for distances in Spriggs et al. (2018).

4 Simulations

The relationship between genetic and geographic dissimilarities in real data can be influenced by a plethora of factors, including sampling scale (Anderson et al., 2010), introgression, i.e., gene flow between distinct species (Bamberger et al., 2021), missingness in the genetic data (Séré et al., 2017), habitat configuration and heterogeneity (Strien et al., 2015), to name just a few. By enabling researchers to control some of these factors, simulations have proved crucial in the related literature (Epperson et al., 2010). Balkenhol et al. (2015, ch. 6) highlights the importance of simulations, particularly individual-based and spatially explicit, in landscape genetics. More than 20 software packages for simulating genome-wide data are listed in Bourgeois and Warren (2021).

The software packages employed in this study simulate genetic data for individuals with geographic locations rather than dissimilarities, see Figure 2. They are based on models for the evolutionary processes that lie behind the modification of the alleles in the loci sampled from the individuals’ DNA. These algorithms simulate the life cycle of individuals that inhabit an artificial map and, generation by generation, exchange their genetic material through migration schemes that give rise to different IBD behaviours. The genetic make-up of the output individuals is the result of this complex set of factors, which will indirectly impact the relationship between genetic and geographic distances.

All tests are run at level $\alpha = 0.05$. In the following, the two simulators used in this comparative study and the corresponding results are described.

4.1 Simulations based on the SLiM simulator

As explained in its user manual (Haller and Messer, 2022), SLiM (Haller and Messer, 2023) is a forward-in-time simulation package for constructing genetically explicit individual-based evolutionary models. Its default settings include non overlapping generations, diploid individuals and offspring generated by recombination of parental chromosomes with the addition of new mutations. Within each species, an arbitrary number of subpopulations can be simulated, connected by any pattern of migration. Individuals can be hermaphroditic or sexual and mating need not be biparental. Mutations at specific base positions in the genomes are explicitly modelled, also as nucleotide sequences.

SLiM provides support for continuous space, either in one, two or three dimensions, and this can help simulate dispersal (mate choice with spatial kernel or nearest-neighbor search) and spatial competition. Importantly, SLiM allows the simulation of more than one species in a single SLiM model, opening the door to ecological interactions and coevolutionary dynamics. Virtually any feature of the simulated evolutionary scenario can be controlled via the integrated Eidos scripting language, which was created specifically for SLiM.

The SLiM manual describes more than 100 scripts (called “recipes”) for simulating particular evolutionary scenarios. The short summary above hints at how its numerous simulation possibilities could be exploited to investigate the type I error rate and power of the methodologies explained in the previous sections. A two-group continuous space simulation, with individuals that compete for foraging areas (resulting in a more likely reproduction of more isolated individuals), choose mates among their nearest neighbors and generate offspring in their surroundings, will lead to observations isolated by distance. Instead, absence of competition and less parent-dependent offspring positioning will lead to quasi-panmictic results, i.e., to the lack of association between genetic and geographic distances. The individuals from the two groups might inhabit the same geographic area or might be segregated into two disjoint areas. As regards the conspecificity and distinctness scenarios:

- a simulation with one species and one subpopulation sampled with an artificial random split will return a naive conspecificity scenario, which can be used as baseline;
- a simulation with only one species and two subpopulations, which descend from the same parent population and are able to exchange migrants, may yield a scenario consistent with the null hypothesis of conspecificity, because the two groups are related by their history and their individuals are expected to display a similar genetic make-up;
- a simulation exploiting SLiM’s multispecies engine (introduced in chapter 19 of the manual), with two distinct species that cannot interact, may generate a scenario consistent with the alternative hypothesis of distinctness, since their genetic information is expected to be completely unrelated.

The details about SLiM’s assumptions and key parameters for the simulations carried out in this study are reported below. The code for the three scenarios above can be found in Appendix C.1.

The simulation was initialized on a two-dimensional map and with an explicit nucleotide sequence 1000 base pairs long: this means that a total of 1000 diploid loci (technically, two genomes with 1000 positions) were simulated, where four different alleles can be found - corresponding to the four nucleobases: adenine, cytosine, guanine and thymine. The initial nucleotide sequence was random and the recombination rate was set to the default low value of 10^{-8} (loci were not independent). Mutations were handled according to the Jukes-Cantor mutational model (Jukes and Cantor, 1969) by specifying a matrix containing the mutation rates from one nucleobase to the other: a unique rate applied to all transitions among nucleobases and in these simulations it was set to 0.0025, a value that is larger than the default: too low values would lead to too few mutations and thus less genetic structure, given the timescale of the simulation. The map was always a square 200×200 units wide, but in any case species were not allowed to get out of the central 100×100 area. As far as mating is concerned, in all scenarios individuals would randomly pick a mate among their three closest neighbors, selected within a circular area of radius 3.

On top of these shared parameter options, the following settings varied according to the scenario:

- in the *split* scenario, throughout the simulation, all individuals inhabited the central 100×100 area. In the conspecificity scenario, the parent population inhabited the central square area, but, depending on the sub-scenarios, the two “children” subpopulations would continue to

share the same wide area (*overlapping conspecific*) or start to migrate to two disjoint areas of the map (*separated conspecific*). By the time of the last simulated generation, the first subpopulation would inhabit the area between point (50, 50) and point (100, 100), whereas the second group would inhabit the area between point (100, 100) and point (150, 150), both included in the original wide central square area. Also in the distinctness scenario there were two sub-scenarios: in the *overlapping distinct* one, both species would inhabit the central 100×100 area, whereas in the *separated distinct* one, they would inhabit, since the very first generation, the area between point (50, 50) and point (100, 100) and the area between point (100, 100) and point (150, 150), respectively.

- In all simulations, SLiM would output the data regarding the individuals only at the last generation. In the *split* scenario, one hundred generations were simulated. In the *conspecificity* scenario, the parent population would be simulated for the first 100 generations and be removed afterwards; the two children subpopulations would originate from the parent one at generation 90 and then be simulated up to generation 150. In the *distinctness* scenario, both species would be simulated for 50 generations.
- The only subpopulation existing in the *split* scenario and the parent population in the *conspecificity* scenario were made up of 400 individuals. The children subpopulations in the *conspecificity* scenario and the two species in the *distinctness* scenario were made up of 200 individuals each. Note that, in each SLiM cycle, individuals are born, mate and die, but the default behaviour of the software is to keep the number of simulated individuals steady throughout the generations.
- In order to generate diverse data richness situations, regardless of the scenario, the number of loci available for the computation of the shared allele distance was either 4, 40 or 89 and the total number of individuals sampled was either 12, 30 or 90. The whole simulation study was carried out either with equally sized groups (e.g., 6 versus 6 individuals) or with one group being twice as large as the other (e.g., 4 versus 8). In the *split* scenario there was just one big group from which individuals were drawn, and these individuals were then randomly assigned to the two groups used to test conspecificity. Given the membership, the drawing of individuals was random, except for the *separated conspecific* scenario, when it was constrained to those individuals inhabiting the subpopulation-specific geographic area of the map: indeed, given the migration process involved in that scenario, it could well happen that some individuals at the last generation were still positioned in the area specific to the other group, typically because one of their parents belonged there.
- As far as spatial competition is concerned, it was modeled through the effect that interactions between individuals had on their probability to reproduce. Each individual experienced an interaction strength that was the sum of all its interactions with individuals in the neighbourhood. In particular, a Gaussian kernel was used to translate the distance between two individuals in the strength of the interaction between them: when trying to enforce a strong IBD behaviour in the individuals, this Gaussian distribution would have mean 2.5 and standard deviation 5 and the interactions with individuals out of the circular area of radius 15 would be set to zero; when trying to mimic no IBD species, the distribution would have mean 0.5 and standard deviation 1 and the circular area with positive-valued interactions would have radius 3. With the first parameter settings, given a certain Euclidean distance between two individuals, the strength of the interaction would be assigned a larger value: the stronger the total interaction felt by an individual, the lower its probability to reproduce, leading to the formation of isolated subgroups and hence to restricted gene flow. With narrower Gaussian

kernels, instead, the total interaction strength on each individual would tend to be smaller and thus there would be less incentive to dispersal, resulting in a more panmictic-like behaviour.

- In the conspecificity scenario, the two children subpopulations were allowed to exchange migrants. A migration rate of 20% means that when creating the offspring for, say, the first subpopulation, 20% of the parents (with some stochastic variability) were picked from individuals belonging to the second subpopulation. In the *overlapping conspecific* scenario, the two subpopulations would exchange parents at a rate randomly oscillating between 40 and 50% till the last generation. In the *separated conspecific* scenario, the migration rate would start off at 20% and then linearly decrease to reach zero in the last generation, at a pace that is consistent with the progressive separation of the geographic areas.
- As far as offspring generation is concerned, it occurred at every simulation cycle after the choice of the two mating parents: its position was shifted from that of the first parent according to a draw from a zero-mean Gaussian kernel with standard deviation 1 in case of strong IBD behaviour and 9 in case of quasi-panmictic behaviour. Thus, with strong spatial competition, the emerging isolated groups would tend to be preserved because offspring were more likely to emerge in a narrow neighbourhood of their parents. In the *separated conspecific* sub-scenario, the location parameter of the Gaussian distribution involved in this process was modified according to the group: for the first group, that would end up in the square area between point (50, 50) and point (100, 100), the parameter was set to -0.5 , whereas it was equal to 0.5 for the second group. Also in this respect, this is consistent with the gradual process of separation that affected the groups since the 100th generation.

In Appendix A, example distance-distance plots similar to Figure 1 from these five scenarios are shown, with equal or unequal group sizes, both for quasi-panmictic groups and for isolated by distance groups.

Results from SLiM As explained above, five scenarios were simulated with SLiM: a *split* scenario (one group, random split), an *overlapping conspecific* scenario (two groups, same parent population, same inhabited area), a *separated conspecific* scenario (two groups, same parent population, disjoint inhabited areas), a *separated distinct* scenario (two species living in disjoint areas) and an *overlapping distinct* scenario (two species inhabiting the same area). Across the scenarios sorted in this way, the rejection rate from species delimitation methods is expected to be non-decreasing, since we transition from a clear conspecificity setup (the *split* strategy) to a clear distinctness setup (the multispecies simulation). On top of these scenarios, other varying parameters (all shared by both groups) were the IBD behaviour and the number of loci available for the computation of \mathbf{D}_y (out of the 1000 loci simulated). In half of the cases the two groups were equally sized and in the other half $n_2 = 2n_1$. The combination of all these factors generated 36 scenarios and in each of them the techniques described in Section 3 were applied both with untransformed and log-transformed geographic distances. One hundred replicates of each of these combinations were generated and the number of rejections was recorded for all the methods. This information is visualized in power plots, one for equal and one for unequal group sizes. In these plots, HH20 denotes the protocol by Hausdorf and Hennig (2020); PMantel denotes PMT with permutations; MJack denotes PMT with jackknife; BC denotes PMT with bias-corrected bootstrap; MXD denotes the mixed effects model (3.9); LM is the multiple regression ignoring dependence.

In Figure 3, rejection rates from the scenarios with equally sized groups are reported (methods' abbreviations are explained in the caption). Results with 40 available loci are only shown in Appendix B, same regarding Section 4.2. The expected non-decreasing trend in the rejection rates

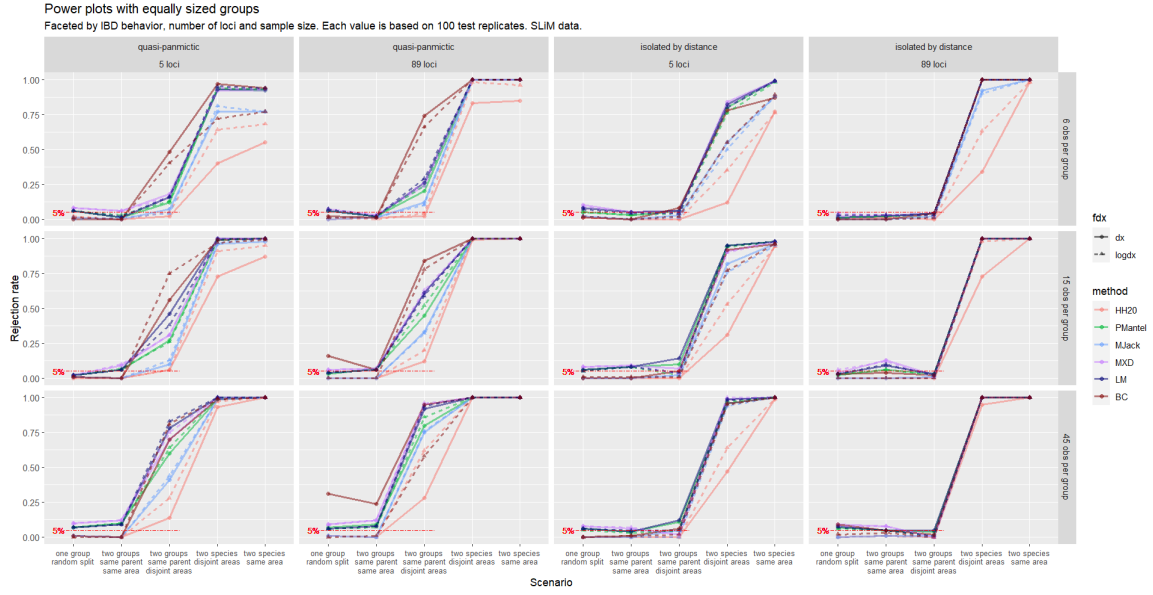


Figure 3: Power plot based on SLiM data simulated **with equally sized groups**. Panels are done by number of individuals per group (rows) and a combination of IBD behavior and number of available loci (columns). Each rejection rate is based on 100 simulations with the same parameter settings. Circles and solid lines refer to analyses with untransformed geographic distances, whereas triangles and dashed lines refer to analyses with log-transformed ones. The horizontal dashed red line is superimposed to help assess type I error rates.

was confirmed, with some minor exceptions between the *split* and the *overlapping conspecific* (same parent, same area) scenario. In the *split* scenario, all methods (surprisingly, model (3.10), too) displayed a type I error rate close to the significance level 5%, although the bias-corrected bootstrap with untransformed \mathbf{D}_x rejected the null hypothesis of conspecificity too often in some setups. In general, the jackknife-based methods (HH20, MJack) showed type I error rates very close to zero, whereas all other methods had them slightly above the significance threshold. In the second scenario, especially with large samples, these methods showed rejection rates close to 10%.

In the *separated conspecific* (same parent, disjoint areas) scenario with quasi-panmictic groups, all rejection rates registered a strong increase: especially with many individuals and loci, all methods seemed to suggest that the two groups should be considered distinct, despite having originated from the same parent population. This was probably due to the combination of geographic separation and absence of IBD behaviour: the genetic structure that was formed because of the decreasing migration rate could not be explained by geographic distance as individuals in the same group tended to be quasi-panmictic. Indeed, when species were isolated by distance and with sufficient genetic information (89 available loci), the rejection rates in the *separated conspecific* scenario all fell below the significance level. Recalling the remark in the Introduction about different levels of biological differentiation, it can be controversial whether the groups generated with this particular SLiM script should be considered conspecific. Most methods concluded they are not, which is important information for biologists using these tests.

Under the multispecies setups, all methods displayed a rejection rate close to 1. The jackknife-

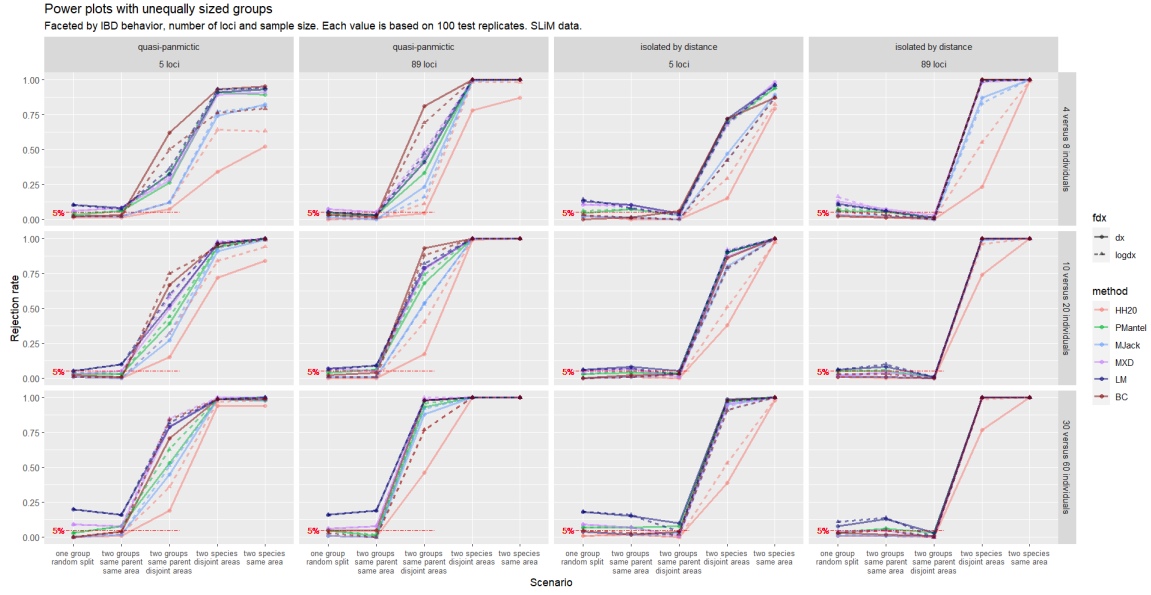


Figure 4: Power plot based on SLiM data simulated with unequally sized groups. See the caption to Figure 3 for further description.

based methods, though, tended to display lower power than the other methods, particularly with small sample sizes. This trend was common to all scenarios: PMantel, MXD, LM and BC always showed rejection rates larger than HH20 and MJack. In this respect, it is worth noting that MJack, representing a compromise between HH20 and PMantel, displayed satisfactory type I error rate and larger power than HH20 in all setups. Now, if the rejection of the null hypothesis in the *split* scenario is seen as a Bernoulli random variable with success probability equal to 0.05, 10 rejections out of 100 would represent a significant result at 5% level. PMantel did not consistently display such significant figures in the simulations, but in an ad hoc simulation under the null hypothesis, with 15 individuals per group and 40 loci (not shown here), this test rejected 70 times out of 1000 repetitions (one-sided p -value = 0.0023 against the null hypothesis that the rejection probability is 0.05). By replacing the permutation-based significance assessment with a jackknife-based one, MJack achieved more power than HH20 while keeping its same low type I error rate. This might support the idea that permutations introduce a distortion in the distribution of geographic distances.

Also in Figure 4, with unequal group sizes, the rejection rates were mostly non-decreasing when going from the *split* scenario to the *overlapping distinct* scenario. The most important difference regards the type I error rate of LM: when one group was twice as large as the other, the rejection rate of LM in the *split* scenario often lay above the significance level, sometimes strongly so, especially with the largest sample sizes.

Regardless of the other parameter options, the transformation of the geographic distances did not seem to have a relevant impact on the methods' performance. The only exception is HH20, whose power increased with log-transformed geographic dissimilarities.

4.2 Simulations based on the GSpace simulator

As clarified in its user manual (Virgoulay et al., 2021a), GSpace (Virgoulay et al., 2021b) is a “a backward generation by generation exact coalescence algorithm with recombination” that allows to simulate allelic data on a lattice under isolation by distance. Each deme on the lattice can represent the locality in population-level simulations or the position of single individuals on the map, approximating continuous habitats. Given the sampled individuals, the history of neutral genes is generated going backward in time and then mutations are simulated from the most recent common ancestor starting from the top of the coalescence tree down to the branches. At each generation, migration is handled by means of two-dimensional dispersal distributions, to be chosen among uniform, geometric, Zeta, etc. Details can be found in Leblois et al. (2009).

As far as the specific settings for the simulations carried out in this study are concerned, a 200×200 demes map was created, with diploid individuals always inhabiting the central 60×60 area. A first group would inhabit the area between point (70, 70) and point (90, 90), whereas a second group would inhabit the square between points (110, 110) and (130, 130). Their coordinates were drawn uniformly within the allowed range. A sequence of di-allelic loci was simulated, with both the mutation rate per generation per locus and the recombination rate per generation between loci equal to 0.005 (ten times the default) for all simulated loci. The so-called K-allele mutation model was used, according to which the initial allelic state is changed into one of the other possible states - in this case the only other allele allowed in the di-allelic setting. In order to mimic a continuous habitat, in each deme there could be up to one individual.

In addition to this, the following parameters varied according to the scenario:

- in order to obtain a baseline scenario where the conspecificity hypothesis was trivially true, the two groups were simulated within the same software execution, so that the algorithm would reconstruct a unique genealogy common to all individuals. In all other cases, the two geographically separated groups were generated during two distinct software executions and collected in the same dataset.
- The two groups would obviously share the same allele pools (the same two allele options for all loci) when generated within the same software execution, whereas they could share both alleles, one allele or no allele otherwise. Of course, when no allele was shared, the genetic dissimilarities between individuals from different groups would always take value one.
- IBD behaviour was controlled via the choice of the univariate dispersal distribution: GSpace assumes that dispersal occurs independently in each dimension. In order to yield panmictic groups, a uniform dispersal was used, according to which the probability of moving t steps in one direction is $\frac{m}{d_{max}}$, where m is the total migration rate, equal to 0.5 and d_{max} is the maximum distance reachable in any migration event, set to 200 (the largest possible value) in all scenarios. As regards IBD species, a Zeta (or truncated discrete Pareto) dispersal distribution was used, assigning value $\frac{m}{2|t|^\kappa}$ to the probability to move t steps in one direction, with $\kappa = 5$ being the shape parameter.
- The total number of simulated individuals was either 12, 30 or 90, whereas the genetic sequence was either 4, 40 or 100 loci long. As with SLiM, all scenarios were investigated both with equally sized groups and with one group twice as large as the other.

Distance-distance plots from all simulated scenarios and the related script can be found in Appendix A and C.2, respectively.

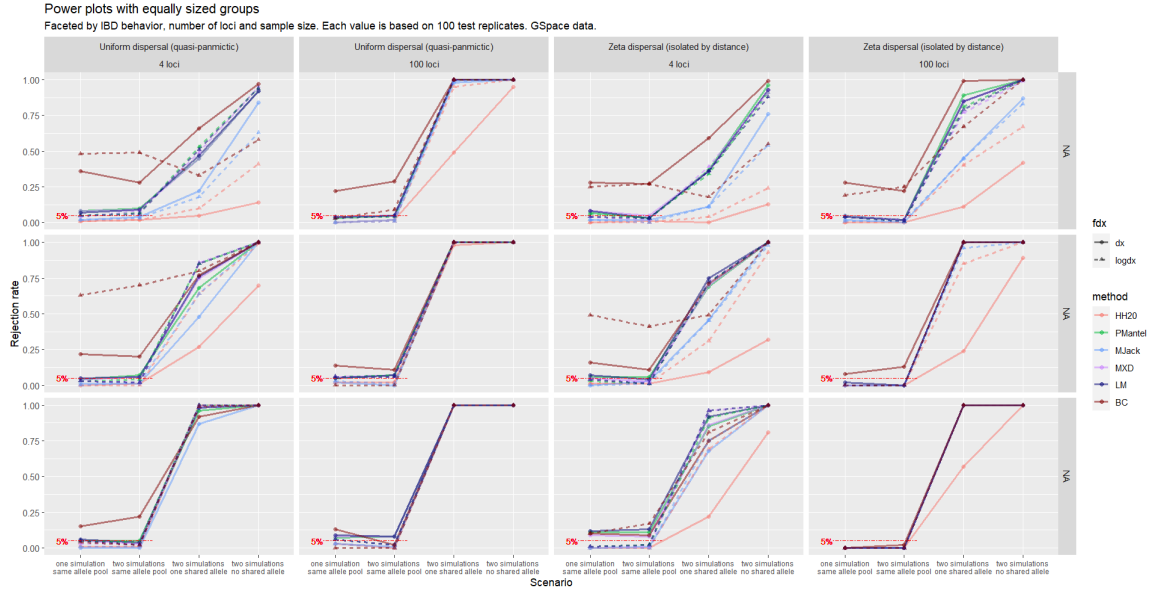


Figure 5: Power plot based on GSpace data simulated with equally sized groups. Panels by combination of IBD behaviour and number of loci (columns) and number of individuals per group (rows). See the caption to Figure 3 for further description.

Results from GSpace The combination of the parameter settings illustrated above led to a total of four scenarios: the simulation involving a unique software execution represented a conspecificity setup, whereas the situation where the allele pools of the two groups shared no allele constituted a distinctness one. The other two setups were included as intermediate situations, with the two groups not sharing ancestors while still showing similarities in their genetic information. Recall that in all these scenarios the geographic separation was always the same: the two groups inhabited two disjoint areas of the map. The four scenarios can be sorted as follows: one execution (*split*), two executions and same alleles (*same allele pool*), two executions and one allele in common (*overlapping allele pools*), two executions and no allele in common (*disjoint allele pools*). In this order, the rejection rate is expected to be non-decreasing.

On top of these scenarios, other varying parameters were the number of individuals per group, the number of loci available for the analysis and the IBD behaviour (absent with Uniform dispersal distribution and strong with Zeta dispersal distribution). Each of these parameter (and scenario) combinations was simulated one hundred times and the number of rejections was recorded.

In Figure 5 the results related to situations in which the two groups are equally sized are reported. It is apparent how the ranking of the methods in terms of performance was similar to that observed in SLiM, apart from the odd behaviour of BC, which displayed very large type I error rates especially with fewer loci and fewer individuals. This is due to resampling with replacement, which led to the emergence of too many zero dissimilarities in the bootstrap samples. A closer look at the related distance-distance plots (not shown here) suggests that these zero dissimilarities were outlying with respect to the bulk of the data, leading to a biased distribution of bootstrap replicates of the partial correlation coefficient. Indeed, accounting for geographic separation, in those situations there appeared to be a large positive association between genetic and grouping distance, as zero distances could only be found when the grouping indicator was equal to zero. Consequently, bootstrap repli-

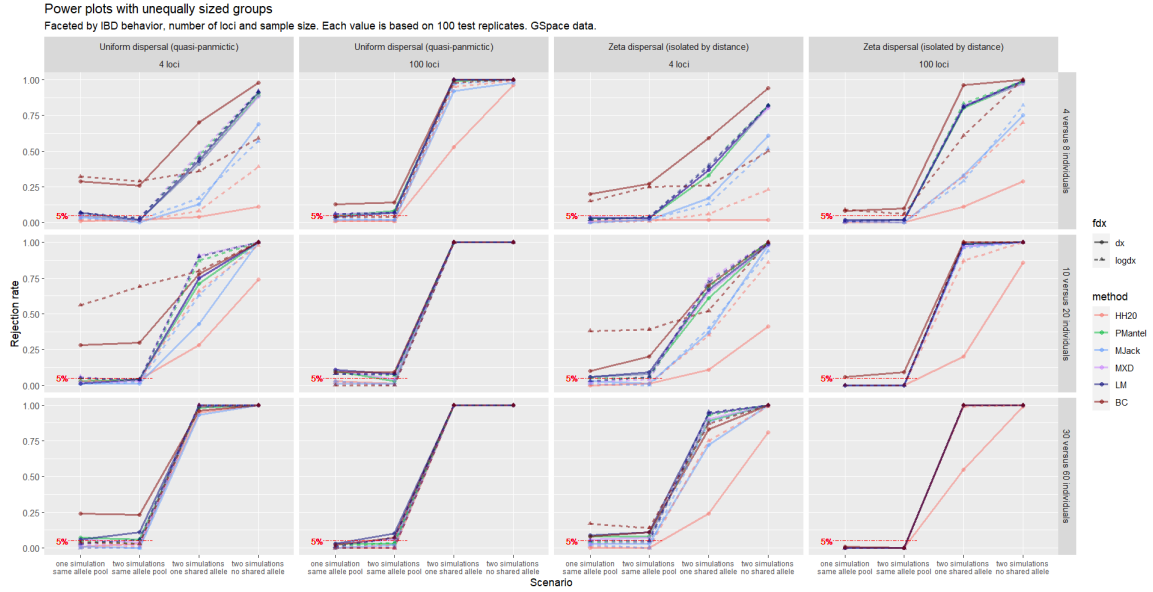


Figure 6: Power plot based on **GSpace** data simulated **with unequal group sizes**. Panels by combination of IBD behaviour and number of loci (columns) and number of individuals per group (rows). See the caption to Figure 3 for further description.

cates had an upward bias that often caused a rejection of the null hypothesis. This phenomenon was not evident with SLiM data because its *split* scenario did not involve geographically separated groups, unlike GSpace. These findings represent empirical evidence that partial Mantel testing with bootstrap can generate unreliable results.

The jackknife-based methods showed lower power with respect to other methods, and once again the logarithmic transformation of \mathbf{D}_x helped HH20 to be more powerful. In the *overlapping allele pools* scenario, given the number of loci and the total sample size, the rejection rates were lower with IBD species than with quasi-panmictic ones. Indeed, with species isolated by distance, geographic separation was sometimes enough to explain the genetic discrepancies between the two groups, and jackknife-based methods were more sensitive to this data feature than other methods.

Figure 6 shows that, when the two groups had unequal sizes, the rejection rates were similar to those with equally sized groups. A slight decrease of some rejection rates across all scenarios can be spotted in the column with IBD species and four loci.

4.3 Discussion

The individual-based spatially-explicit simulations carried out via SLiM and GSpace allowed to study the type I error rate and power of the techniques described in the **Methods** section. A consistent ranking in the overall performance of the methodologies could be observed, with jackknife-based methods being very conservative and not very powerful and the other techniques being more powerful, sometimes at the cost of empirical type I error rates above the significance level.

By combining jackknife significance assessment and the usage of partial correlation coefficients, MJack managed to achieve larger power with respect to HH20, while showing type I error rates consistently beneath the significance level, unlike PMantel. The bias-corrected bootstrap-based

PMT showed a too large type I error rate in the most challenging data setups. No method apart from HH20 clearly benefited from the logarithmic transformation of the geographic distances.

Despite wrongly assuming that all dissimilarities in the dataset are independent, OLS estimation in model (3.10) displayed good type I error rate and power in several situations. In particular, it often performed better than the random effects model MXD, avoiding certain increased type I error probabilities of the latter. However, with SLiM data, the type I error rate of LM was consistently above the significance level when unequally sized groups were being compared. This is in line with the expectation that ignoring the dependence between distances might lead to an underestimation of variability.

The performance of HH20 was summarized by a unique rejection rate in the power plots, but recall that this method is hierarchical. In our study, a rejection corresponded to cases when either H_{02} or H_{03} was rejected, and thus, non-rejections included also the inconclusive results that can arise when testing H_{03} . Although in all simulations both groups always had the same IBD behaviour, some rejections of H_{01} occurred, so that H_{03} rather than H_{02} was tested. The possibility to take into consideration unequal IBD behaviour is unique to HH20, but here may have led to a degradation of its performance. More precisely, lower rejection rates may have been recorded here in spite of the fact that, in some unclear cases, a practitioner could have concluded that two distinct species were being compared.

5 Analysis of brassy ringlets data

Gratton et al. (2016) discussed the biological delimitation of a taxon of butterflies (brassy ringlets; *Erebia tyndarus* complex, Lepidoptera) endemic to Southern Europe, the Altai Republic and the Rocky Mountains. They studied the morphological, genetic and geographic information of 45 individuals netted during the summer of 2012 across the Italian Apennines, the Alps and the Pyrenees. Four subgroups of this clade were represented in the sample, namely *E. Tyndarus*, *E. Nivalis*, *E. Calcaria* and *E. Cassioides*, with the latter possibly divisible in three populations according to the area of collection. After selecting a subset of 389 diploid loci, they applied k-means clustering on the principal components obtained from the genetic data, Bayesian model-based clustering using the STRUCTURE software (Pritchard et al., 2000) and coalescent-based Bayes factor delimitation (Leaché et al., 2014), integrating their results by examining the isolation by distance behaviour and morphological differentiation of the individuals in each putative cluster. The study in Gratton et al. (2016) did not only back up the distinction between the four groups mentioned above from a genetic point of view, but also supported further differentiation within the *Cassioides* group among the Eastern and Orobian Alps population, the Southern and Central Apennines population and the population inhabiting Northern Apennines, Pyrenees and Western Alps.

Hausdorf and Hennig (2020) applied their testing protocol to these data in order to replicate and deepen the IBD investigation carried out by Gratton et al. (2016). With the exclusion of the *Calcaria* group, which could not be examined due to the small sample size (only 3 specimens), the distinction among the groups was confirmed. The classification within the *Cassioides* group, instead, was slightly amended: HH20 suggested that there was no evidence of distinctness between the Southern and Central Apennines population and the population inhabiting Northern Apennines, Pyrenees and Western Alps, whereas the genetic dissimilarity between these populations taken together and the Eastern and Orobian Alps population was too large to be explained by isolation by distance.

In Table 1, the results from all methods involved in this study are reported. See Figure 1 for the dissimilarity data on which three of these comparisons are based. The only non-rejections of the null hypothesis of conspecificity occurred for *E. Cassioides*: W_Alps + Pyrenees + N_Apennines

Table 1: Results from all methods compared here on the brassy ringlets data. For the three tests in HH20, p-values are reported (two of them are given for H_{03} when discordant); p-values are reported for PMantel, MJack and LM, too; for MXD and BC, confidence intervals are reported for the b_2^* regression coefficient and the partial correlation coefficient, respectively: if their lower boundary is larger than zero, the null hypothesis is rejected.

Groups compared	H_{01}	H_{02}	H_{03}	PMantel	MJack	MXD	LM	BC
<i>E. Tyndarus</i> vs <i>E. Nivalis</i>	0.074	$< 10^{-5}$	n.a.	0.001	$< 10^{-29}$	(0.296, 0.306)	$< 10^{-113}$	(0.983, 0.995)
<i>E. Nivalis</i> vs <i>E. Cassioides</i>	0.094	$< 10^{-4}$	n.a.	0.001	$< 10^{-55}$	(0.378, 0.389)	~ 0	(0.972, 0.988)
<i>E. Tyndarus</i> vs <i>E. Cassioides</i>	$< 10^{-9}$	n.a.	both $< 10^{-24}$	0.001	$< 10^{-67}$	(0.345, 0.352)	~ 0	(0.977, 0.986)
<i>E. Cassioides</i> : W.Alps + Pyrenees + N.Apennines vs Orobian + E.Alps	0.487	0.004	n.a.	0.001	$< 10^{-5}$	(0.025, 0.036)	$< 10^{-17}$	(0.493, 0.745)
<i>E. Cassioides</i> : W.Alps + Pyrenees + N.Apennines vs Central + S.Apennines	$< 10^{-4}$	n.a.	0.098; 0.004	0.002	0.015	(0.030, 0.045)	$< 10^{-5}$	(-0.148, 0.552)
<i>E. Cassioides</i> : Central + S.Apennines vs Orobian + E.Alps	0.144	0.009	n.a.	0.001	$< 10^{-4}$	(0.041, 0.066)	$< 10^{-15}$	(0.477, 0.484)
<i>E. Cassioides</i> : W.Alps + Pyrenees + ALL Apennines vs Orobian + E.Alps	1	$< 10^{-4}$	n.a.	0.001	$< 10^{-8}$	(0.020, 0.029)	$< 10^{-25}$	(0.329, 0.618)

vs Central + S.Apennines (middle panel in Figure 1) by the bias-corrected bootstrap-based Partial Mantel test (the CI contains 0) and the larger one of the two group-wise p-values for H_{03} by HH20.

In all other cases, all methods agreed upon the distinctness results, confirming the conclusions shared by Gratton et al. (2016) and Hausdorf and Hennig (2020) - including also the distinction between the Western and Apennines populations versus the Eastern and Orobian populations (last row in Table 1). According to the evidence collected in this study, not only the *E. Tyndarus*, *E. Nivalis* and *E. Cassioides* groups should be considered distinct: also the three subgroups identified within the *E. Cassioides* group, namely the Eastern and Orobian Alps population, the Southern and Central Apennines population and the population inhabiting Northern Apennines, Pyrenees and Western Alps, display a genetic structure that cannot be explained by their geographic separation.

6 Conclusions

We investigated methods that model the relationship between genetic and geographic dissimilarities in biological species in order to perform species delimitation. These techniques check whether the genetic structure existing between two putative species is compatible with the way genetic dissimilarities within each group increase with the geographic separation of the individuals. The type I error rate and power of these methods were compared by means of individual-based simulations carried out with the simulators GSpace and SLiM. Results showed that the method of Hausdorf and Hennig (2020) (HH20) has a type I error rate close to zero and lower power than Partial Mantel tests (PMTs) as applied by Medrano et al. (2014), which in turn had type I error rates slightly above the significance level in some setups. Testing PMTs with jackknife instead of permutations fixed this behaviour, ensuring more power than HH20 while keeping the type I error rate still close to zero. Testing PMTs with bias-corrected bootstrap confidence intervals, instead, often led to inflated type I error rates. The linear mixed effects model displayed a performance similar to PMT. A linear regression without random effects (LM), i.e., wrongly assuming independence among the

dissimilarities, showed inflated type I error rates only with unequally sized groups simulated with SLiM, and performed surprisingly well otherwise.

The ranking in the overall performance of the methods was consistent over both simulators, and the log-transformation of the geographic dissimilarities did not seem to have a considerable impact on methods other than HH20, where it improved matters.

Due to the extremely large amount of possibilities defined by parameter choices of the simulators, many more potentially interesting situations could be simulated. Some scenarios worth exploring could involve comparisons between groups with different IBD behaviour, size and separation of the inhabited areas, but also simulations with independent loci, different settings for the time scale and migration rates, etc. Moreover, the investigation could be extended to population-based simulations, using genetic dissimilarity measures like F_{st} (Weir and Cockerham, 1984) or the chord distance (Cavalli-Sforza and Edwards, 1967). The individual-based methods compared in this study often assume independence between observations in the same group, something that is not biologically grounded and is indeed avoided in population-based studies.

In addition, another simulation-based investigation could be set up in order to compare the performance of these methods in scenarios where there is no putative grouping known in advance. To this end, an automated unsupervised routine for species delimitation may be conceived that uses the tests investigated here to decide whether groups that come out of a cluster analysis produced by methods such as STRUCTURE (Pritchard et al., 2000) should be merged. The conSTRUCT approach (Bradburd et al., 2018) does something similar, but is only applicable when the number of loci is much larger than n , whereas, as shown in this study, most methods investigated here worked fairly good even with very small n and P .

Applying the methods treated here to other problems of regression between dissimilarities such as relating similarity between languages or dialects to geographic distance (Bella et al., 2021) may also be of interest.

References

- Adriaensen, F., J.P. Chardon, G. De Blust, E. Swinnen, S. Villalba, H. Gulinck, and E. Matthysen (2003). “The application of ‘least-cost’ modelling as a functional landscape model”. In: *Landscape and Urban Planning* 64.4, pp. 233–247. DOI: [https://doi.org/10.1016/S0169-2046\(02\)00242-6](https://doi.org/10.1016/S0169-2046(02)00242-6).
- Anderson, Corey Devin, Bryan K Epperson, Marie-Josée Fortin, Rolf Holderegger, Patrick MA James, Michael S Rosenberg, Kim T Scribner, and Stephen Spear (2010). “Considering spatial and temporal scale in landscape-genetic studies of gene flow”. In: *Molecular Ecology* 19.17, pp. 3565–3575.
- Balkenhol, Niko, Samuel Cushman, and Andrew Storfer (2015). *Landscape Genetics: Concepts, Methods, Applications*. Newark: Wiley, pp. 1–264.
- Bamberger, Sonja, Jie Xu, and Bernhard Hausdorf (2021). “Evaluating Species Delimitation Methods in Radiations: The Land Snail *Albinaria cretensis* Complex on Crete”. In: *Systematic Biology* 71.2, pp. 439–460. DOI: [10.1093/sysbio/syab050](https://doi.org/10.1093/sysbio/syab050).
- Bates, Douglas, Martin Mächler, Ben Bolker, and Steve Walker (2015). “Fitting Linear Mixed-Effects Models Using lme4”. In: *Journal of Statistical Software* 67.1, pp. 1–48. DOI: [10.18637/jss.v067.i01](https://doi.org/10.18637/jss.v067.i01).
- Bella, Gabor, Khuyagbaatar Batsuren, and Fausto Giunchiglia (2021). “A Database and Visualization of the Similarity of Contemporary Lexicons”. In: *Proceedings of the 24th International*

- Conference on Text, Speech, and Dialogue, Olomouc, Czech Republik*. Ed. by Kamil Ekstein, Frantisek Partl, and Miloslav Konopik. Springer Nature, Switzerland, pp. 95–104.
- Bourgeois, Yann XC and Ben H Warren (2021). “An overview of current population genomics methods for the analysis of whole-genome resequencing data in eukaryotes”. In: *Molecular Ecology* 30.23, pp. 6036–6071.
- Bowcock, A. M, A Ruiz-Linares, J Tomfohrde, E Minch, J. R Kidd, and L. L Cavalli-Sforza (1994). “High resolution of human evolutionary trees with polymorphic microsatellites”. In: *Nature (London)* 368.6470, pp. 455–457.
- Bradburd, Gideon S., Graham M. Coop, and Peter L. Ralph (2018). “Inferring Continuous and Discrete Population Genetic Structure Across Space”. In: *Genetics* 210.1, pp. 33–52. DOI: [10.1534/genetics.118.301333](https://doi.org/10.1534/genetics.118.301333).
- Burbrink, Frank T. and Sara Ruane (2021). “Contemporary Philosophy and Methods for Studying Speciation and Delimiting Species”. In: *Ichthyology & Herpetology* 109.3, pp. 874–894. DOI: [10.1643/h2020073](https://doi.org/10.1643/h2020073).
- Carstens, Bryan C, Tara A Pelletier, Noah M Reid, and Jordan D Satler (2013). “How to fail at species delimitation”. In: *Molecular Ecology* 22.17, pp. 4369–4383.
- Cavalli-Sforza, L L and A W Edwards (1967). “Phylogenetic analysis. Models and estimation procedures”. In: *American journal of human genetics* 19.3 Pt 1, pp. 233–257.
- Cayuela, Hugo, Quentin Rougemont, Jérôme G. Prunier, Jean-Sébastien Moore, Jean Clobert, Aurélien Besnard, and Louis Bernatchez (2018). “Demographic and genetic approaches to study dispersal in wild animal populations: A methodological review”. In: *Molecular Ecology* 27.20, pp. 3976–4010.
- Clarke, Ralph T, Peter Rothery, and Alan F Raybould (2002). “Confidence limits for regression relationships between distance matrices: estimating gene flow with distance”. In: *Journal of Agricultural, Biological, and Environmental Statistics* 7.3, pp. 361–372.
- De Queiroz, Kevin (2007). “Species Concepts and Species Delimitation”. In: *Systematic Biology* 56.6, pp. 879–886. DOI: [10.1080/10635150701701083](https://doi.org/10.1080/10635150701701083).
- Edwards, Danielle L and L Lacey Knowles (2014). “Species detection and individual assignment in species delimitation: can integrative data increase efficacy?” In: *Proceedings of the Royal Society B: Biological Sciences* 281.1777, p. 20132765.
- Efron, Bradley and Robert J. Tibshirani (1993). *An introduction to the bootstrap*. New York London: Chapman & Hall.
- Epperson, Bryan K., Brad H. McRae, Kim Scribner, Samuel A. Cushman, Michael S. Rosenberg, Marie-Josée Fortin, Patrick M. A. James, Melanie Murphy, Stéphanie Manel, Pierre Legendre, and Mark R. T. Dale (2010). “Utility of computer simulations in landscape genetics”. In: *Molecular Ecology* 19.17, pp. 3549–3564. DOI: <https://doi.org/10.1111/j.1365-294X.2010.04678.x>.
- Frantz, A. C., S. Cellina, A. Krier, L. Schley, and T. Burke (2009). “Using spatial Bayesian methods to determine the genetic structure of a continuously distributed population: clusters or isolation by distance?” In: *Journal of Applied Ecology* 46.2, pp. 493–505. DOI: <https://doi.org/10.1111/j.1365-2664.2008.01606.x>.
- Goslee, Sarah C and Dean L Urban (2007). “The ecodist package for dissimilarity-based analysis of ecological data”. In: *Journal of Statistical Software* 22, pp. 1–19.
- Gratton, Paolo, Emiliano Trucchi, Alessandra Trasatti, Giorgio Riccarducci, Silvio Marta, Giuliana Allegrucci, Donatella Cesaroni, and Valerio Sbordoni (2016). “Testing Classical Species Properties with Contemporary Data: How ”Bad Species” in the Brassy Ringlets (*Erebia tyndarus* complex, Lepidoptera) Turned Good”. In: *Systematic Biology* 65.2, pp. 292–303.

- Haller, Benjamin C and Philipp W Messer (2023). “SLiM 4: multispecies eco-evolutionary modeling”. In: *The American Naturalist* 201.5, E127–E139.
- (2022). *SLiM Manual*. URL: <https://messerlab.org/slim/> (visited on 12/07/2023).
- Hausdorf, Bernhard (2011). “Progress toward a general species concept”. In: *Evolution* 65.4, pp. 923–931. DOI: [10.1111/j.1558-5646.2011.01231.x](https://doi.org/10.1111/j.1558-5646.2011.01231.x).
- Hausdorf, Bernhard and Christian Hennig (2019). *Package ‘prabclus’, version 2.3-2*. URL: <https://CRAN.R-project.org/package=prabclus> (visited on 07/25/2023).
- (2020). “Species delimitation and geography”. In: *Molecular Ecology Resources* 20.4, pp. 950–960. DOI: <https://doi.org/10.1111/1755-0998.13184>.
- Hutchison, Delbert W. and Alan R. Templeton (1999). “Correlation of Pairwise Genetic and Geographic Distance Measures: Inferring the Relative Influences of Gene Flow and Drift on the Distribution of Genetic Variability”. In: *Evolution* 53.6, pp. 1898–1914.
- Ishida, Yoichi (2009). “Sewall Wright and Gustave Malécot on Isolation by Distance”. In: *Philosophy of Science* 76.5, pp. 784–796.
- Jukes, Thomas H. and Charles R. Cantor (1969). “Chapter 24 - Evolution of Protein Molecules”. In: *Mammalian Protein Metabolism*. Ed. by H.N. Munro. Academic Press, pp. 21–132. DOI: <https://doi.org/10.1016/B978-1-4832-3211-9.50009-7>.
- Kimura, Motoo and G. H. Weiss (1964). “The Stepping Stone Model of Population Structure and the Decrease of Genetic Correlation with Distance”. In: *Genetics (Austin)* 49.4, pp. 561–576.
- Leaché, Adam D., Matthew K. Fujita, Vladimir N. Minin, and Remco R. Bouckaert (2014). “Species Delimitation using Genome-Wide SNP Data”. In: *Systematic Biology* 63.4, pp. 534–542.
- Leblois, Raphaël, Arnaud Estoup, and Francois Rousset (2009). “IBDSim: a computer program to simulate genotypic data under isolation by distance”. In: *Molecular Ecology Resources* 9.1, pp. 107–109.
- Legendre, Pierre (2000). “Comparison of permutation methods for the partial correlation and partial Mantel tests”. In: *Journal of statistical computation and simulation* 67.1, pp. 37–73.
- Legendre, Pierre and Louis Legendre (2012). *Numerical ecology*. 3rd English ed.. Developments in environmental modelling ; 24. Amsterdam ; Boston: Elsevier.
- MacDonald, Zachary G., Julian R. Dupuis, Corey S. Davis, John H. Acorn, Scott E. Nielsen, and Felix A. H. Sperling (2020). “Gene flow and climate-associated genetic variation in a vagile habitat specialist”. In: *Molecular Ecology* 29.20, pp. 3889–3906. DOI: <https://doi.org/10.1111/mec.15604>.
- Mantel, Nathan (1967). “The Detection of Disease Clustering and a Generalized Regression Approach”. In: *Cancer Research* 27.2 Part 1, pp. 209–220.
- McRae, Brad H. (2006). “Isolation by Resistance”. In: *Evolution* 60.8, pp. 1551–1561.
- McRae, Brad H., Brett G Dickson, Timothy H. Keitt, and Viral B. Shah (2008). “Using Circuit Theory to model connectivity in Ecology, Evolution and Conservation”. In: *Ecology (Durham)* 89.10, pp. 2712–2724.
- Medrano, Mónica, Esmeralda López-Perea, and Carlos M Herrera (2014). “Population Genetics Methods Applied to a Species Delimitation Problem: Endemic Trumpet Daffodils (*Narcissus-SectionPseudonarcissi*) from the Southern Iberian Peninsula”. In: *International journal of plant sciences* 175.5, pp. 501–517.
- Meirmans, Patrick G. (2012). “The trouble with isolation by distance”. In: *Molecular Ecology* 21.12, pp. 2839–2846. DOI: <https://doi.org/10.1111/j.1365-294X.2012.05578.x>.
- Peterman, William E. (2018). “ResistanceGA: An R package for the optimization of resistance surfaces using genetic algorithms”. In: *Methods in Ecology and Evolution* 9.6, pp. 1638–1647. DOI: <https://doi.org/10.1111/2041-210X.12984>.

- Peterman, William E. and Nathaniel S. Pope (2021). “The use and misuse of regression models in landscape genetic analyses”. In: *Molecular Ecology* 30.1, pp. 37–47. DOI: <https://doi.org/10.1111/mec.15716>.
- Pritchard, Jonathan K, Matthew Stephens, and Peter Donnelly (2000). “Inference of Population Structure Using Multilocus Genotype Data”. In: *Genetics (Austin)* 155.2, pp. 945–959.
- Rannala, Bruce and Ziheng Yang (2020). “Species delimitation”. In: ed. by C Scornavacca, F Delsuc, and N Galtier. Self published.
- Raxworthy, Christopher J, Colleen M Ingram, Nirhy Rabibisoa, and Richard G Pearson (2007). “Applications of Ecological Niche Modeling for Species Delimitation: A Review and Empirical Evaluation Using Day Geckos (*Phelsuma*) from Madagascar”. In: *Systematic Biology* 56.6, pp. 907–923. DOI: [10.1080/10635150701775111](https://doi.org/10.1080/10635150701775111).
- Rissler, Leslie J. and Joseph J. Apodaca (2007). “Adding More Ecology into Species Delimitation: Ecological Niche Models and Phylogeography Help Define Cryptic Species in the Black Salamander (*Aneides flavipunctatus*)”. In: *Systematic Biology* 56.6, pp. 924–942. DOI: [10.1080/10635150701703063](https://doi.org/10.1080/10635150701703063).
- Rousset, François (1997). “Genetic Differentiation and Estimation of Gene Flow from F-Statistics Under Isolation by Distance”. In: *Genetics* 145.4, pp. 1219–1228. DOI: [10.1093/genetics/145.4.1219](https://doi.org/10.1093/genetics/145.4.1219).
- (2008). “genepop’007: a complete re-implementation of the genepop software for Windows and Linux”. In: *Molecular Ecology Resources* 8.1, pp. 103–106. DOI: <https://doi.org/10.1111/j.1471-8286.2007.01931.x>.
- Royston, Patrick (2007). “Profile likelihood for estimation and confidence intervals”. In: *The Stata Journal* 7.3, pp. 376–387.
- SAS Institute (2001). *SAS/STAT user’s guide. Ver. 8*. Cary, NC.
- Scapini, Felicita, Andrea Aloia, Mohamed F Bouslama, Lorenzo Chelazzi, Isabella Colombini, Mohamed ElGtari, Mario Fallaci, and Giovanni M. Marchetti (2002). “Multiple regression analysis of the sources of variation in orientation of two sympatric sandhoppers, *Talitrus saltator* and *Talorchestia brito*, from an exposed Mediterranean beach”. In: *Behavioral Ecology and Sociobiology* 51, pp. 403–414.
- Séré, M, S Thévenon, A M G Belem, and T De Meeûs (2017). “Comparison of different genetic distances to test isolation by distance between populations”. In: *Heredity* 119.2, pp. 55–63.
- Shirk, Andrew J., Erin L. Landguth, and Samuel A. Cushman (2018). “A comparison of regression methods for model selection in individual-based landscape genetic analysis”. In: *Molecular Ecology Resources* 18.1, pp. 55–67. DOI: <https://doi.org/10.1111/1755-0998.12709>.
- Slatkin, Montgomery (1993). “Isolation by Distance in Equilibrium and Non-Equilibrium Populations”. In: *Evolution* 47.1, pp. 264–279.
- Smouse, Peter E., Jeffrey C. Long, and Robert R. Sokal (1986). “Multiple Regression and Correlation Extensions of the Mantel Test of Matrix Correspondence”. In: *Systematic Zoology* 35.4, pp. 627–632.
- Spriggs, Elizabeth L, Deren A R Eaton, Patrick W Sweeney, Caroline Schlutius, Erika J Edwards, and Michael J Donoghue (2018). “Restriction-Site-Associated DNA Sequencing Reveals a Cryptic *Viburnum* Species on the North American Coastal Plain”. In: *Systematic Biology* 68.2, pp. 187–203. DOI: [10.1093/sysbio/syy084](https://doi.org/10.1093/sysbio/syy084).
- Storfer, Andrew, Melanie A Murphy, Stephen F Spear, Rolf Holderegger, and Lisette P Waits (2010). “Landscape genetics: where are we now?” In: *Molecular Ecology* 19.17, pp. 3496–3514.
- Strien, M J van, R Holderegger, and H J Van Heck (2015). “Isolation-by-distance in landscapes: considerations for landscape genetics”. In: *Heredity* 114.1, pp. 27–37.

- Székely, Gábor J., Maria L. Rizzo, and Nail K. Bakirov (2007). “Measuring and testing dependence by correlation of distances”. In: *The Annals of Statistics* 35.6, pp. 2769–2794. DOI: [10.1214/009053607000000505](https://doi.org/10.1214/009053607000000505).
- Van Strien, Maarten J., Daniela Keller, and Rolf Holderegger (2012). “A new analytical approach to landscape genetic modelling: least-cost transect analysis and linear mixed models”. In: *Molecular Ecology* 21.16, pp. 4010–4023.
- Vekemans, X. and O. J. Hardy (2004). “New insights from fine-scale spatial genetic structure analyses in plant populations”. In: *Molecular Ecology* 13.4, pp. 921–935. DOI: <https://doi.org/10.1046/j.1365-294X.2004.02076.x>.
- Venzon, DJ and SH Moolgavkar (1988). “A method for computing profile-likelihood-based confidence intervals”. In: *Journal of the Royal Statistical Society: Series C (Applied Statistics)* 37.1, pp. 87–94.
- Virgoulay, Thimothée, François Rousset, and Raphaël Leblois (2021a). *GSpace User Guide*. URL: https://www1.montpellier.inrae.fr/CBGP/software/gspace/ressources/documentation/GSpace_User_Guide.pdf (visited on 12/07/2023).
- (2021b). “GSpace: an exact coalescence simulator of recombining genomes under isolation by distance”. In: *Bioinformatics* 37.20, pp. 3673–3675.
- Wang, Ian J. and Gideon S. Bradburd (2014). “Isolation by environment”. In: *Molecular Ecology* 23.23, pp. 5649–5662.
- Weir, B. S. and C. Clark Cockerham (1984). “Estimating F-Statistics for the Analysis of Population Structure”. In: *Evolution* 38.6, pp. 1358–1370.
- Welch, B. L. (1947). “The generalization of ‘Student’s’ problem when several different population variances are involved”. In: *Biometrika* 34.1-2, pp. 28–35. DOI: [10.1093/biomet/34.1-2.28](https://doi.org/10.1093/biomet/34.1-2.28).
- West, Brady T, Kathleen B Welch, and Andrzej T Galecki (2022). *Linear mixed models: a practical guide using statistical software*. Crc Press.
- Yang, Rong-Cai (2004). “A Likelihood-based approach to estimating and testing for isolation by distance”. In: *Evolution* 58.8, pp. 1839–1845. DOI: <https://doi.org/10.1111/j.0014-3820.2004.tb00466.x>.

A Dissimilarity-dissimilarity plots

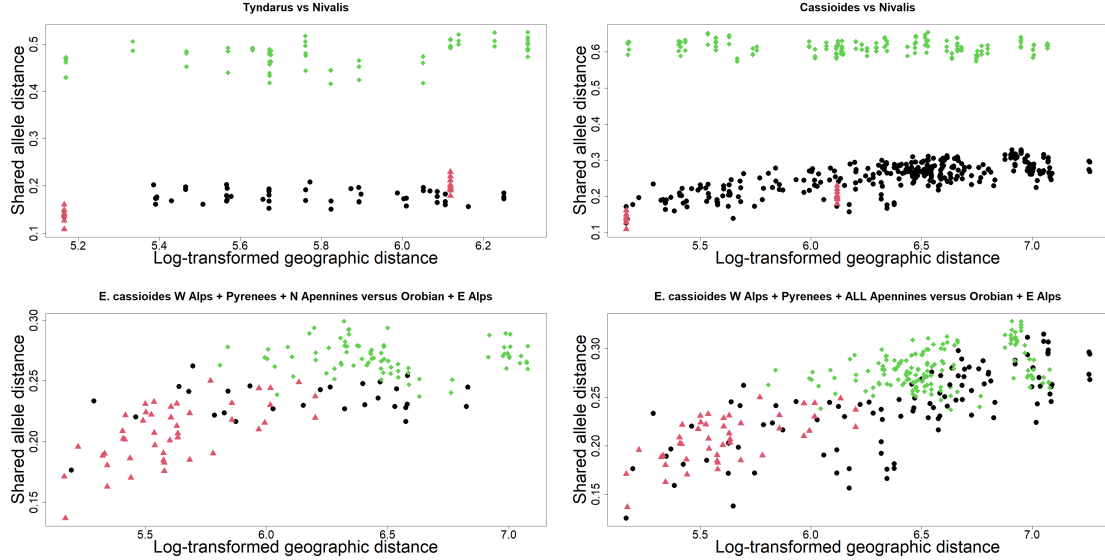


Figure 7: Log-transformed geographic distances vs. Shared allele distances for the four pairs of groups indicated in Table 1 but not shown in Figure 1 of the main text from the brassy ringlets data. The black circles (first group) and red triangles (second group) show distances between pairs of individuals belonging to the same group. The green diamonds show the distances between two individuals belonging to different groups.

Figure 7 shows the corresponding visualisations for the four pairs of groups of the brassy ringlets data that were tested in Table 1 of the main text but not shown in Figure 1 of the main text.

In Figure 8, the shared allele distance is plotted against the log-transformed geographic distance for a random dataset from each of the five scenarios simulated by SLiM with equal-sized groups and without IBD behaviour. It is easy to see that, by colour, there was no association between genetic and geographic dissimilarities. The *split* and the *overlapping conspecific* scenarios are similar, with the latter displaying a larger variability in the genetic dissimilarities. In the third scenario, the geographic separation can be clearly seen by the range of the green-colored points. In the multispecies scenarios (bottom row), the range of the between-group genetic dissimilarities was always above that of the within-group ones, supporting distinctness: models that fit an update in the intercept to a linear regression of \mathbf{D}_y against \mathbf{D}_x easily caught this trend in the data.

In Figure 9, similar dissimilarity-dissimilarity plots are shown for IBD species with equal sample sizes. It is apparent how the shared allele distance is positively correlated with geographic distance as far as individuals close in space are considered, but this trend soon plateaus and dissimilarities never take values larger than around 0.9 (also in the quasi-panmictic datasets). This saturation causes a convexity in the relationship that is not fixed by the logarithmic transformation of the geographic distances. Also in this chart it is easy to notice: a) how within and between-group dissimilarities are separated in the *distinct* scenarios and b) how the IBD behaviour is common to both groups.

In Figures 10 and 11, the same kind of plots are shown for setups where the two groups had unequal sample sizes. It is easy to see that there are fewer black points than red ones: more

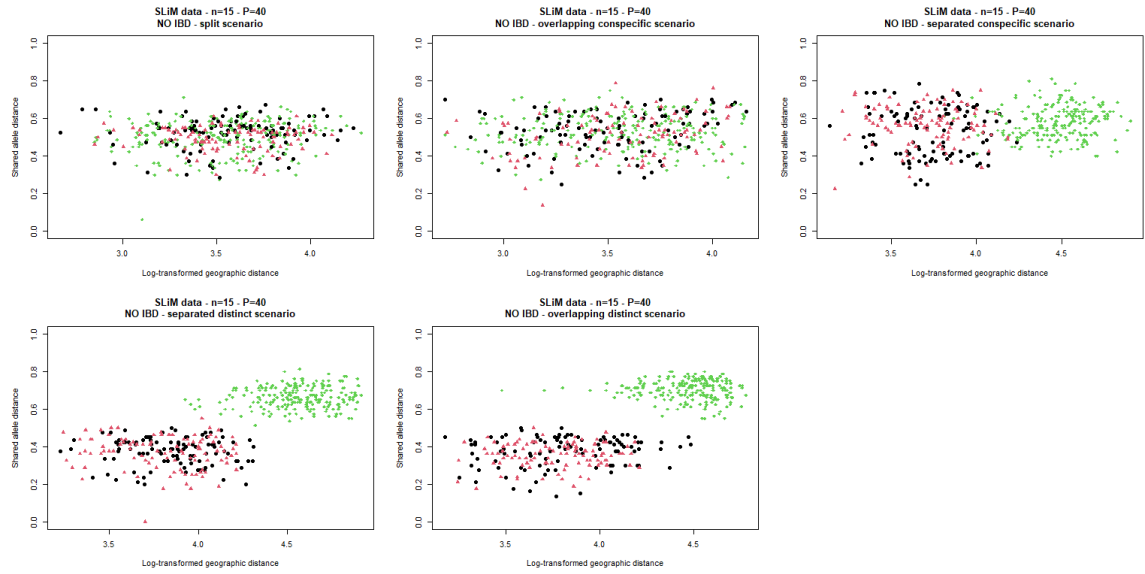


Figure 8: Distance-distance plots (shared allele distance against log-transformed geographic distance) from the five scenarios simulated with **SLiM**, **without IBD behaviour**, **15 individuals per group** and 40 available loci. Each scenario is specified in the plot title. In black the dissimilarities among individuals belonging to the first group, in red those for the second group and in green the dissimilarities among individuals belonging to different groups.

precisely, given that $n_1 = 10$ and $n_2 = 20$, there are 45 black circles and 190 red triangles in each plot; between-groups dissimilarities (green diamonds) are 200.

In Figure 12, the shared allele distance is plotted against the log-transformed geographic distance for a random dataset from each of the four scenarios simulated by GSpace without IBD behaviour. As expected, there is no association between genetic and geographic dissimilarities within the groups. The *split* and *same allele pool* scenarios look rather similar and a major difference with respect to SLiM distinctness setups lies in the range of the dissimilarities among individuals belonging to different groups: in the *disjoint allele pool* scenario, since the genetic make-ups in the two groups are completely different, all genetic dissimilarities take value 1.

In Figure 13, the same visualizations are provided for species displaying a positive association between genetic and geographic dissimilarities. This relationship is however harder to spot with respect to SLiM simulations as it seems to relate only a small share of the individuals in the two groups. In both Figures, the between-group genetic dissimilarities in the *overlapping allele pool* scenario are centered around the value 0.75, whereas in all scenarios the bulk of the within-group shared allele distances is centered at 0.5. This vertical shift in the genetic dissimilarities, which is even stronger in the last scenario, could be quite effectively captured by an update in the intercept of the linear models fitted on this data.

In Figures 14 and 15, similar plots from GSpace simulations with same parameter options as above but unequal-sized groups are reported. In scenarios with very small sample sizes, it could well happen that the available dissimilarities were not enough to express a positive IBD behavior even with Zeta dispersal (see, e.g., the black group in the top-left plot of Figure 15).

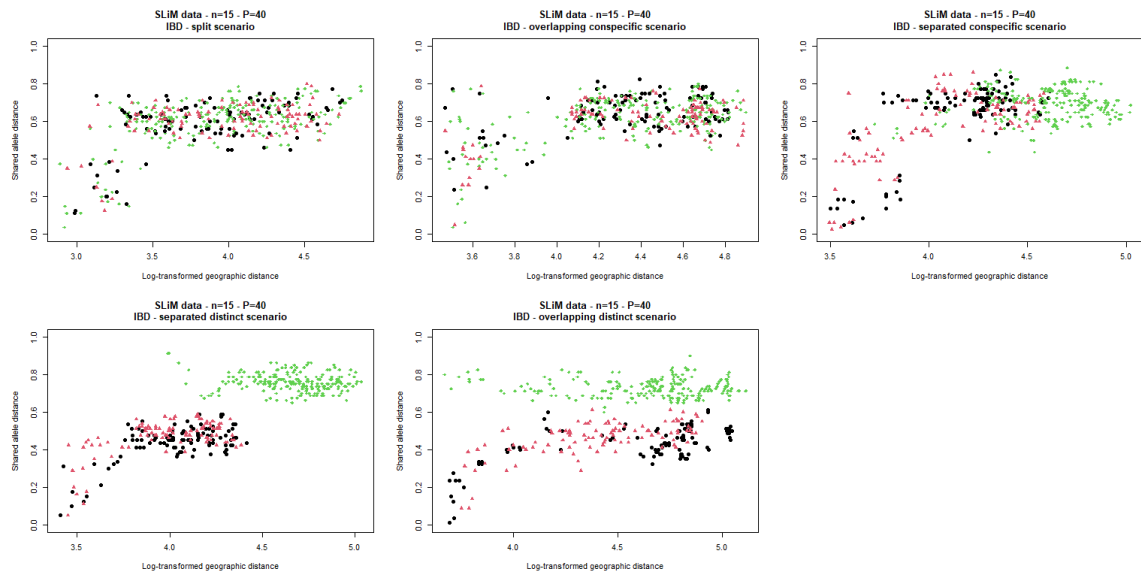


Figure 9: Distance-distance plots (shared allele distance against log-transformed geographic distance) from the five scenarios simulated with **SLiM**, with **IBD** behaviour, **15 individuals per group** and **40 available loci**.

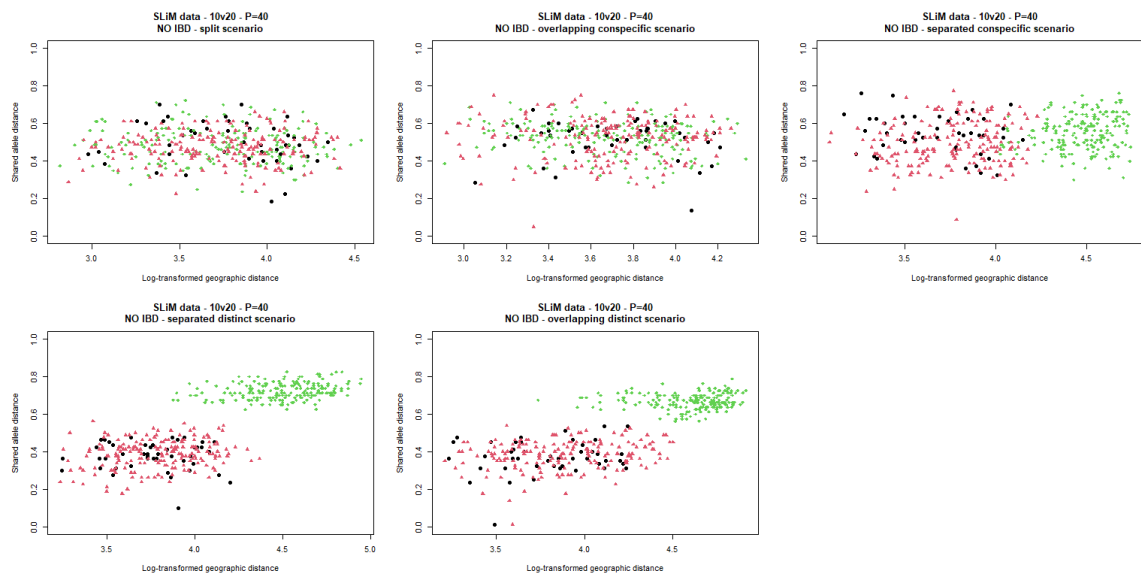


Figure 10: Distance-distance plots (shared allele distance against log-transformed geographic distance) from the five scenarios simulated with **SLiM**, without **IBD** behaviour, **10 versus 20 individuals** and **40 available loci**.

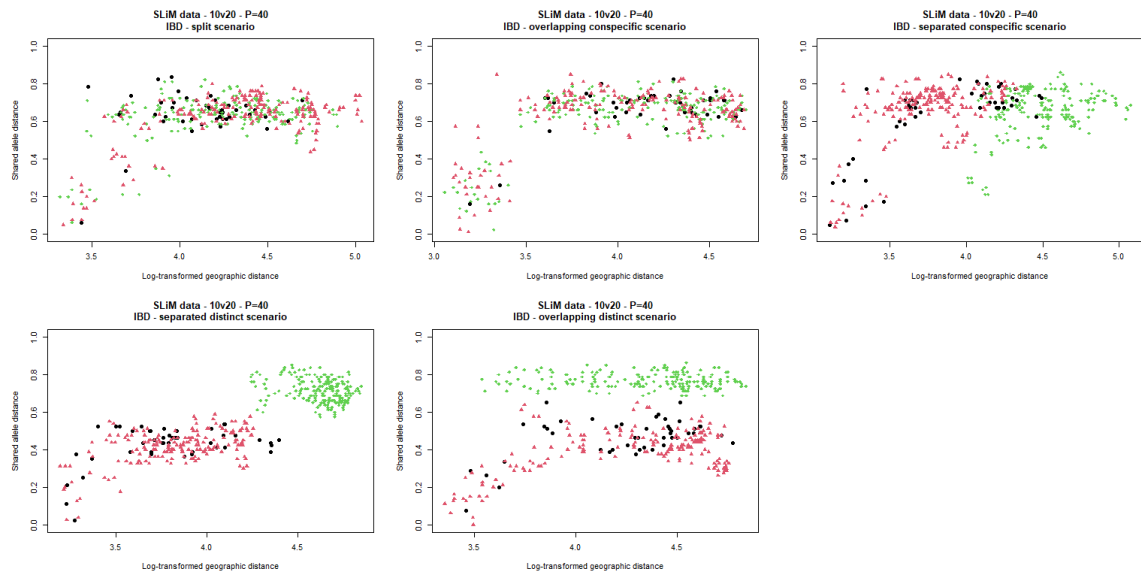


Figure 11: Distance-distance plots (shared allele distance against log-transformed geographic distance) from the five scenarios simulated with **SLiM**, with **IBD** behaviour, **10 versus 20 individuals** and **40 available loci**.

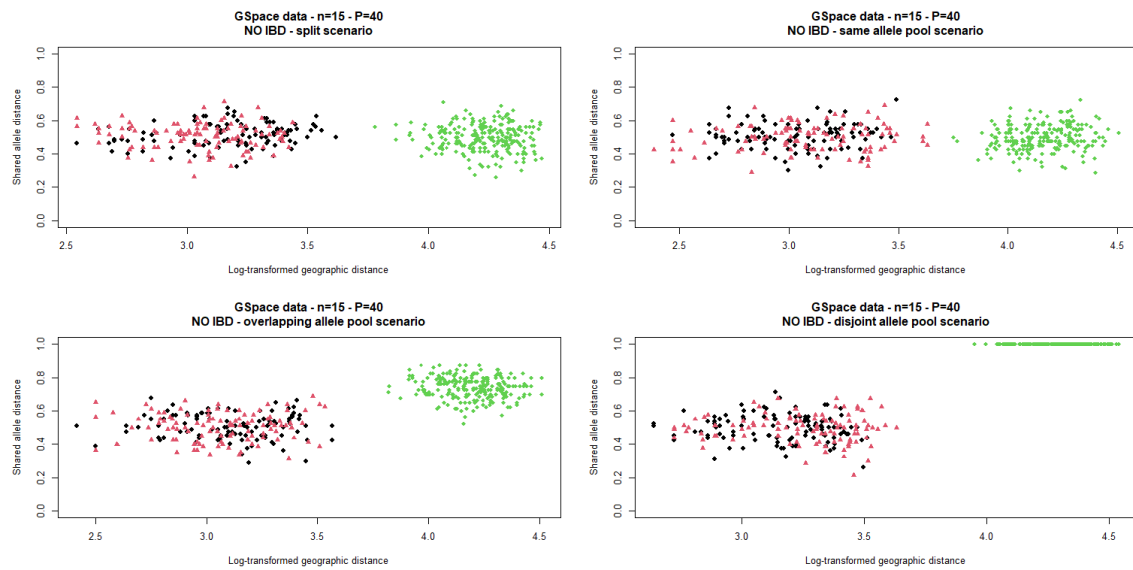


Figure 12: Distance-distance plots (shared allele distance against log-transformed geographic distance) from the four scenarios simulated with **GSpace**, without **IBD** behaviour, with **15 individuals per group** and **40 available loci**.

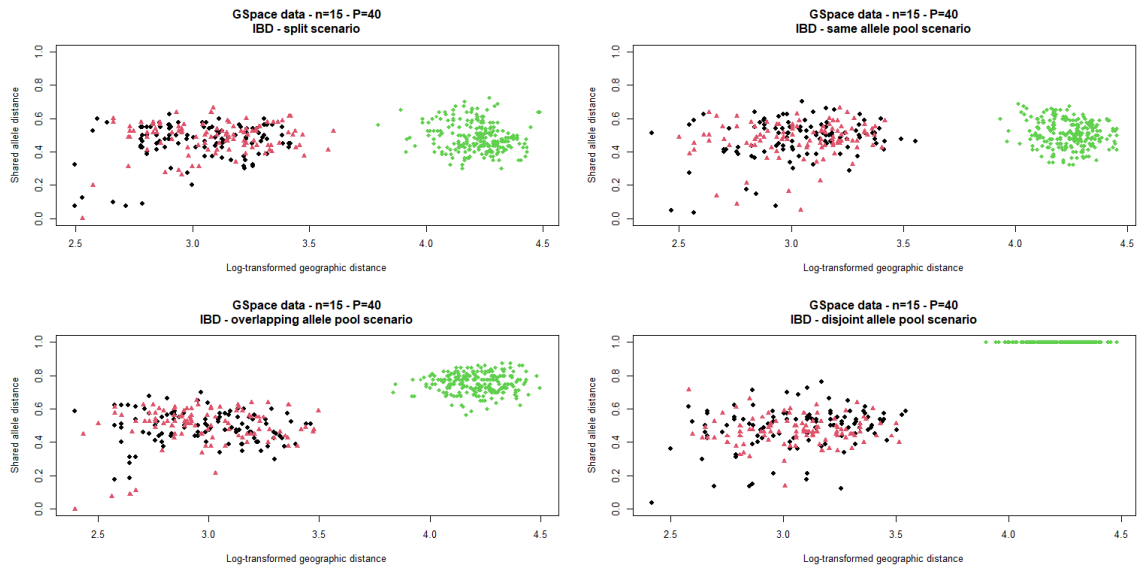


Figure 13: Distance-distance plots (shared allele distance against log-transformed geographic distance) from the four scenarios simulated with **GSpace**, with **IBD** behaviour, **15 individuals per group** and **40 available loci**.

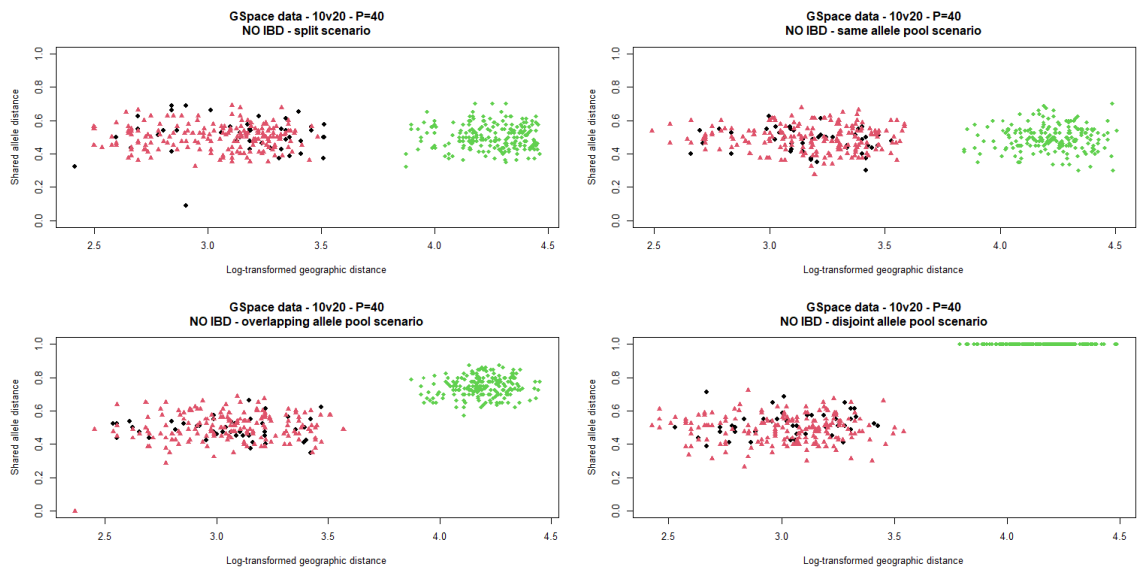


Figure 14: Distance-distance plots (shared allele distance against log-transformed geographic distance) from the four scenarios simulated with **GSpace**, without **IBD** behaviour, with **10 versus 20 individuals** and **40 available loci**.

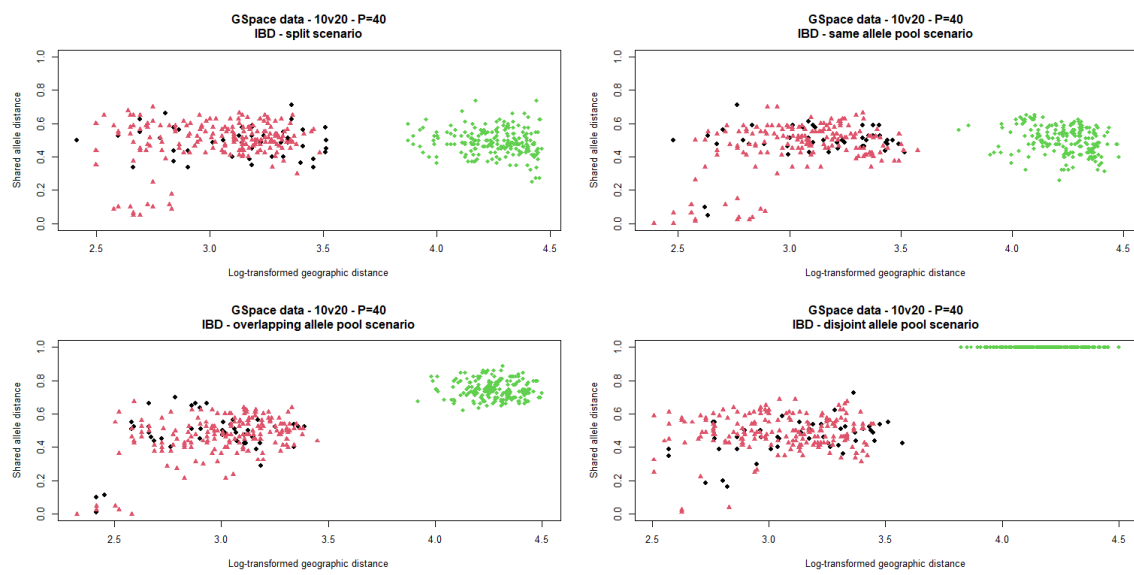


Figure 15: Distance-distance plots (shared allele distance against log-transformed geographic distance) from the four scenarios simulated with **GSpace**, with **IBD** behaviour, **10 versus 20 individuals** and **40 available loci**.

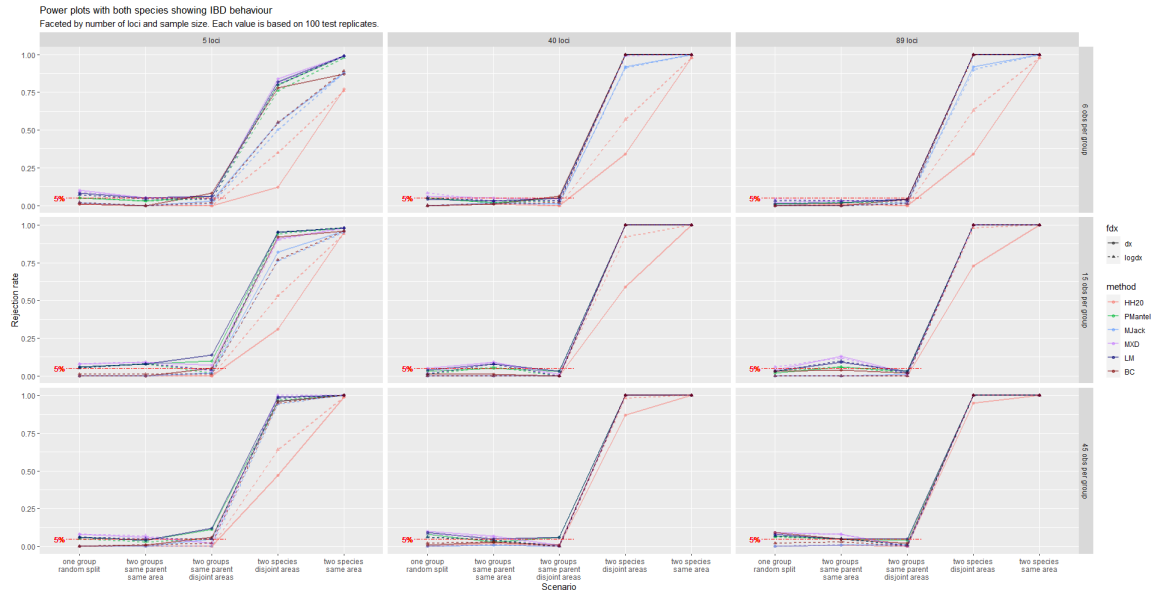


Figure 17: Power plot based on SLiM data simulated with equal-sized isolated by distance groups. See the caption to Figure 16 for further description.

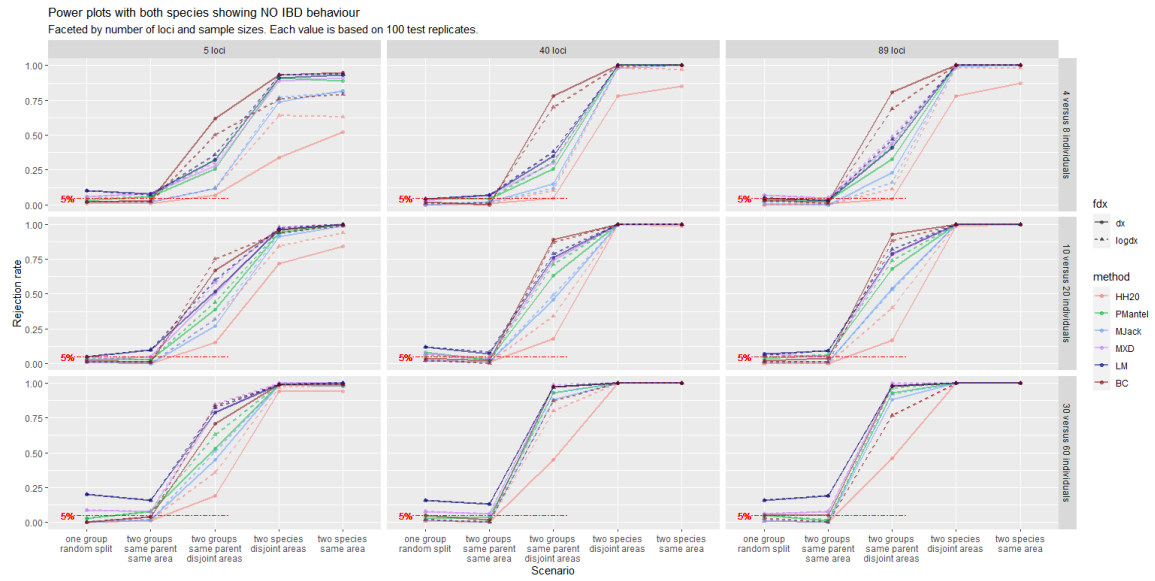


Figure 18: Power plot based on SLiM data simulated with unequal-sized quasi-panmictic groups. See the caption to Figure 16 for further description.

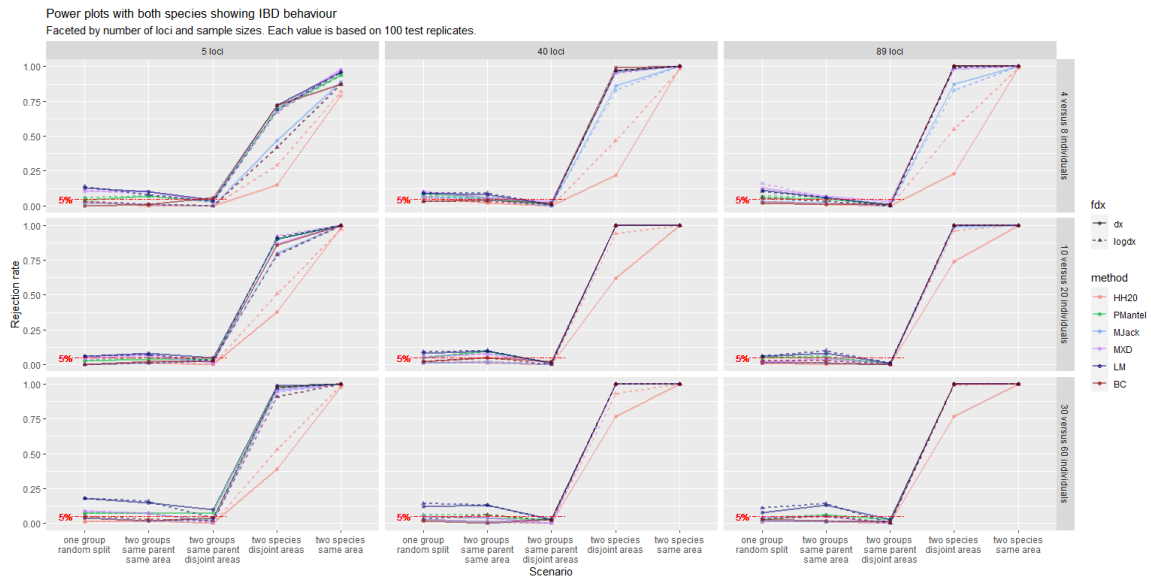


Figure 19: Power plot based on SLiM data simulated with unequal-sized isolated by distance groups. See the caption to Figure 16 for further description.

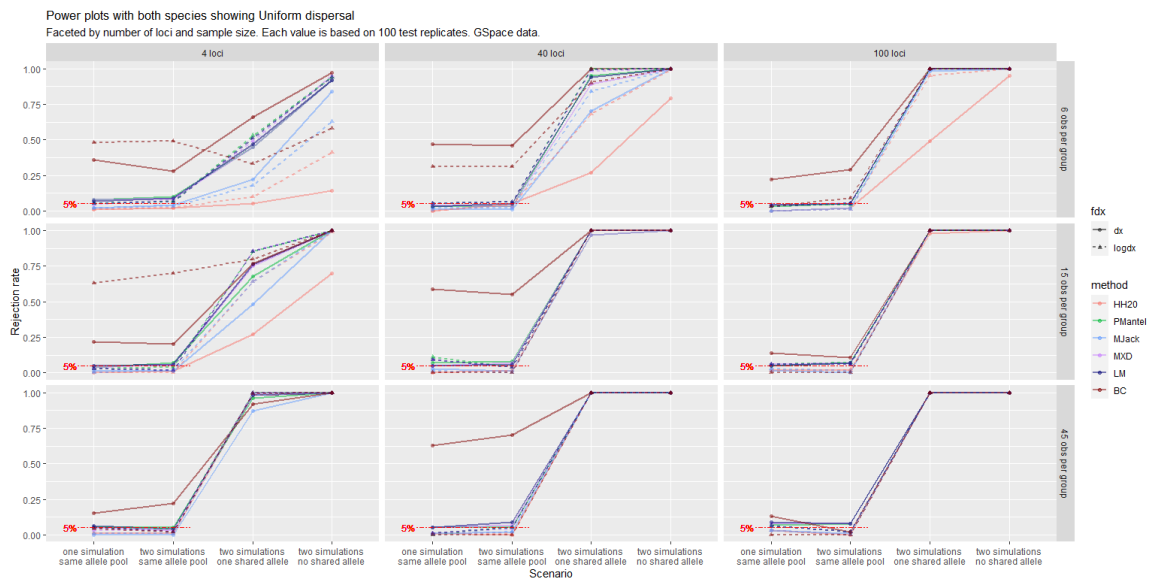


Figure 20: Power plot based on GSpace data simulated with equal-sized quasi-panmictic groups. See the caption to Figure 16 for further description.

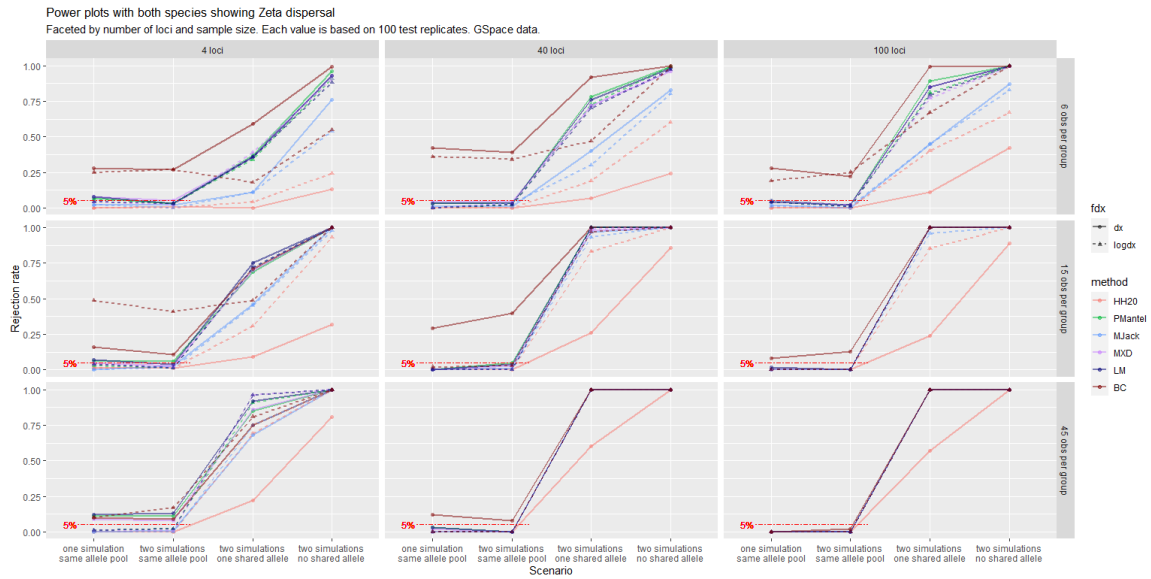


Figure 21: Power plot based on GSpace data simulated with equal-sized isolated by distance groups. Facets by number of individuals per group (rows) and number of available loci (columns). See the caption to Figure 16 for further description.

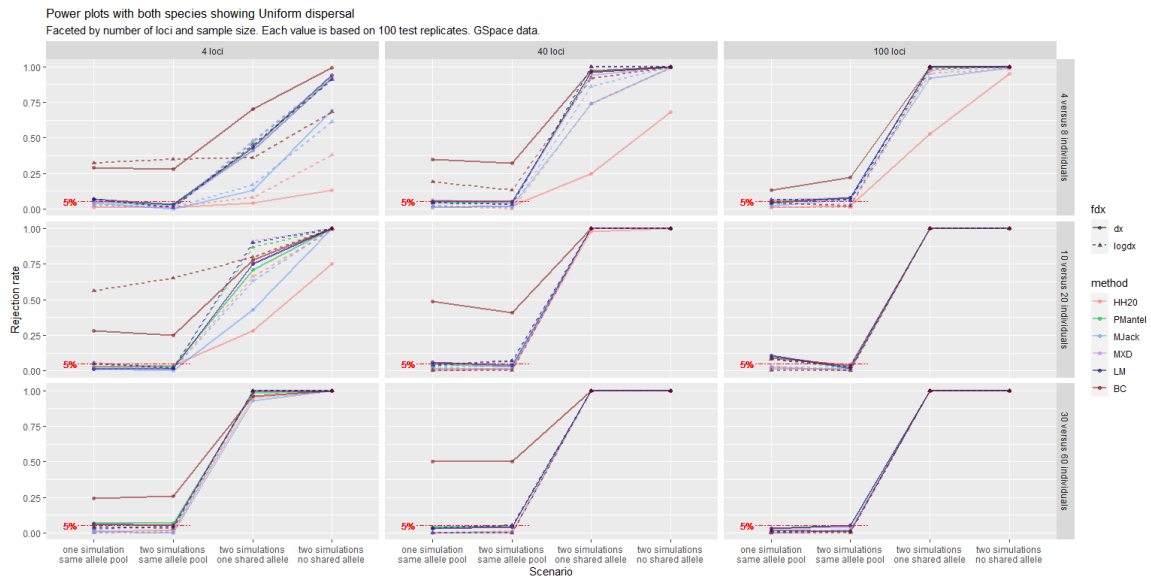


Figure 22: Power plot based on GSpace data simulated with unequal-sized quasi-panmictic groups. See the caption to Figure 16 for further description.

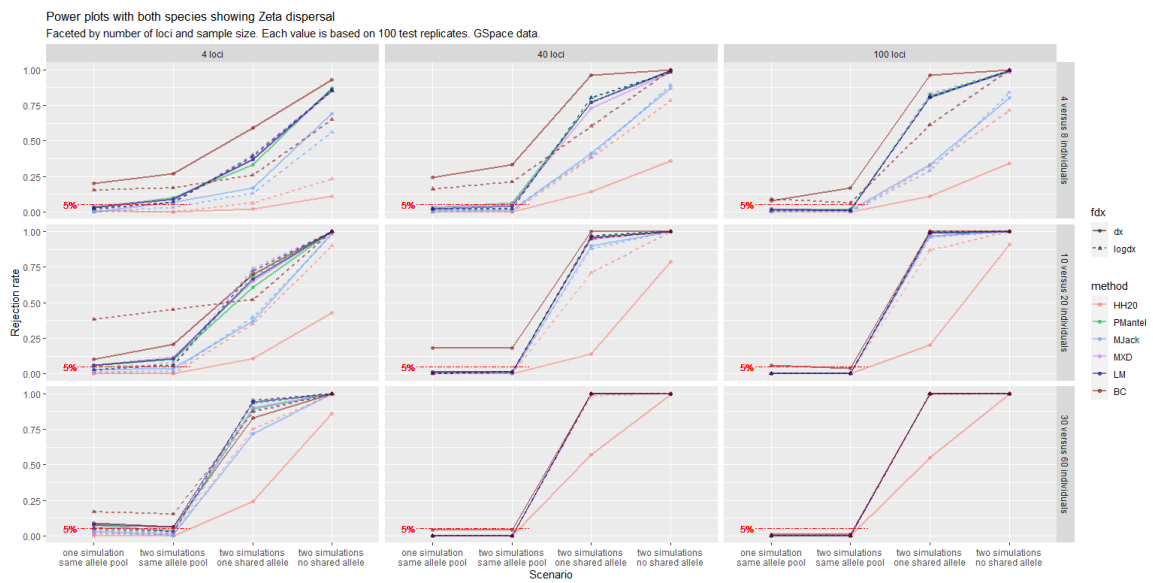


Figure 23: Power plot based on **GSpace** data simulated with unequal-sized isolated by distance groups. See the caption to Figure 16 for further description.

C Software code

C.1 SLiM

Script editing, software executions and data analysis were carried out in R. The variables defined with the `defineConstant` command were set at each simulation iteration before feeding the script to the SLiM executable: for instance, `i1sd` would take value 1 or 5 according to the scenario at hand.

Listing 1: SLiM script for the *split* scenario

```
1 initialize() {
2 initializeSLiMOptions(keepPedigrees = T, dimensionality="xy", nucleotideBased=T);
3   defineConstant("L", 1e3);
4   initializeAncestralNucleotides(randomNucleotides(L));
5   initializeMutationTypeNuc("m1", 0.5, "f", 0.0);
6   initializeGenomicElementType("g1", m1, 1.0, mmJukesCantor(2.5e-3));
7   initializeGenomicElement(g1, 0, L-1);
8   initializeRecombinationRate(rates = 1e-8);
9
10  defineConstant(symbol="nsim", value=200);
11  defineConstant(symbol="nsam", value=45);
12  defineConstant(symbol="i1sd", value=1);
13  defineConstant(symbol="i2maxd", value=3);
14  defineConstant(symbol="nneigh", value=3);
15  defineConstant(symbol="childsd", value=9);
16
17  // spatial competition
18  initializeInteractionType(1, "xy", reciprocal=T, maxDistance=3*i1sd);
19  i1.setInteractionFunction("n", i1sd/2, i1sd);
20
21
22  // spatial mate choice
23  initializeInteractionType(2, "xy", reciprocal=T, maxDistance=i2maxd);
24 }
25
26 1 late() {
27   sim.addSubpop("p0", nsim*2);
28   p0.setSpatialBounds(c(50.00, 50.00, 150.00, 150.00));
29   p0.individuals.setSpatialPosition(p0.pointUniform(nsim*2));
30 }
31
32 1:100 late() {
33   i1.evaluate(p0);
34   inds = p0.individuals;
35   competition = i1.totalOfNeighborStrengths(inds) / size(inds);
36   competition = pmin(competition, 0.99);
37   inds.fitnessScaling = 1 - competition;
38 }
39
40 2:100 first() {
41   i2.evaluate(p0);
42 }
43
44 mateChoice(p0) {
45   // nearest-neighbor mate choice
46   neighbors = i2.nearestNeighbors(individual, count = nneigh);
47   return (size(neighbors) ? sample(neighbors, 1) else float(0));
48 }
49 modifyChild(p0) {
```

```

50     do pos = parent1.spatialPosition + rnorm(2, 0, childsd);
51     while (!p0.pointInBounds(pos));
52     child.setSpatialPosition(pos);
53
54     return T;
55 }
56
57 100 late() { // last generation
58     sampledIndividuals = p0.sampleIndividuals(nsam*2);
59
60     out = paste("subpopulation", "pedigreeID", "x", "y", "genome1", "genome2");
61     for (i in sampledIndividuals){
62         info = paste(i.subpopulation, i.pedigreeID, i.spatialPosition, i.genome1.
63             nucleotides(), i.genome2.nucleotides());
64         out = c(out, info);
65     }
66     writeFile("coordgenomes.txt", out);
67 }

```

Listing 2: SLiM script for the *conspecificity* scenario

```

1 initialize() {
2     initializeSLiMOptions(keepPedigrees = T, dimensionality="xy", nucleotideBased=T);
3     defineConstant("L", 1e3);
4     initializeAncestralNucleotides(randomNucleotides(L));
5     initializeMutationTypeNuc("m1", 0.5, "f", 0.0);
6     initializeGenomicElementType("g1", m1, 1.0, mmJukesCantor(2.5e-3));
7     initializeGenomicElement(g1, 0, L-1);
8     initializeRecombinationRate(rates = 1e-8);
9
10    defineConstant(symbol="nsim", value=200);
11    defineConstant(symbol="nsam", value=45);
12    defineConstant(symbol="i1sd", value=1);
13    defineConstant(symbol="i2maxd", value=3);
14    defineConstant(symbol="nneigh", value=3);
15    defineConstant(symbol="childsd", value=9);
16    defineConstant(symbol="separation", value=F);
17
18    // spatial competition
19    initializeInteractionType(1, "xy", reciprocal=T, maxDistance=3*i1sd);
20    i1.setInteractionFunction("n", i1sd/2, i1sd);
21
22    // spatial mate choice
23    initializeInteractionType(2, "xy", reciprocal=T, maxDistance=i2maxd);
24 }
25 1 late() {
26     sim.addSubpop("p0", nsim*2);
27     p0.setSpatialBounds(c(50.00, 50.00, 150.00, 150.00));
28     p0.individuals.setSpatialPosition(p0.pointUniform(nsim*2));
29 }
30
31 1:100 late() {
32     i1.evaluate(p0);
33     inds = p0.individuals;
34     competition = i1.totalOfNeighborStrengths(inds) / size(inds);
35     competition = pmin(competition, 0.99);
36     inds.fitnessScaling = 1 - competition;
37 }
38 2:100 first() { i2.evaluate(p0); }
39

```

```

40 90 early() {
41     sim.addSubpopSplit("p1", nsim, p0);
42     sim.addSubpopSplit("p2", nsim, p0);
43     p1.setSpatialBounds(c(50.00, 50.00, 150.00, 150.00));
44     p2.setSpatialBounds(c(50.00, 50.00, 150.00, 150.00));
45     p1.individuals.setSpatialPosition(p1.pointUniform(nsim));
46     p2.individuals.setSpatialPosition(p2.pointUniform(nsim));
47 }
48
49 91: late() {
50     i1.evaluate(p1);
51     inds = p1.individuals;
52     competition = i1.totalOfNeighborStrengths(inds) / size(inds);
53     competition = pmin(competition, 0.99);
54     inds.fitnessScaling = 1 - competition;
55
56     i1.evaluate(p2);
57     inds = p2.individuals;
58     competition = i1.totalOfNeighborStrengths(inds) / size(inds);
59     competition = pmin(competition, 0.99);
60     inds.fitnessScaling = 1 - competition;
61 }
62
63 92: first() {
64     i2.evaluate(p1);
65     i2.evaluate(p2);
66 }
67
68 101 early() { p0.setSubpopulationSize(0); }
69
70
71 101:150 early() {
72     if(separation){
73     p1.setSpatialBounds(p1.spatialBounds + c(0, 0, -1, -1));
74     p2.setSpatialBounds(p2.spatialBounds + c(1, 1, 0, 0));
75     }
76 }
77
78 92: early() {
79     migrationProgress = runif(1, min=0.8, max=1);
80     p1.setMigrationRates(p2, 0.5 * migrationProgress);
81     p2.setMigrationRates(p1, 0.5 * migrationProgress);
82 }
83
84
85 // NEAREST NEIGHBORS MATE CHOICE
86 2:91 mateChoice(p0) {
87     // nearest-neighbor mate choice
88     neighbors = i2.nearestNeighbors(individual, count = nneigh);
89     return (size(neighbors) ? sample(neighbors, 1) else float(0));
90 }
91 2:91 modifyChild(p0) {
92     do pos = parent1.spatialPosition + rnorm(2, 0, childsd);
93     while (!p0.pointInBounds(pos));
94     child.setSpatialPosition(pos);
95     return T;
96 }
97
98 92: mateChoice(p1) {
99     // nearest-neighbor mate choice

```

```

100     neighbors = i2.nearestNeighbors(individual, count = nneigh);
101     return (size(neighbors) ? sample(neighbors, 1) else float(0));
102 }
103 92: mateChoice(p2) {
104     // nearest-neighbor mate choice
105     neighbors = i2.nearestNeighbors(individual, count = nneigh);
106     return (size(neighbors) ? sample(neighbors, 1) else float(0));
107 }
108
109 92: modifyChild(p1) {
110     counter = 1;
111     do{
112         pos = parent1.spatialPosition + rnorm(2, ifelse(separation, -0.5, 0.0),
113             childsd);
114         counter = counter + 1;
115     }
116     while (!p1.pointInBounds(pos) & counter < 100);
117     child.setSpatialPosition(pos);
118     return T;
119 }
120 92: modifyChild(p2) {
121     counter = 1;
122     do{
123         pos = parent1.spatialPosition + rnorm(2, ifelse(separation, 0.5, 0.0),
124             childsd);
125         counter = counter + 1;
126     }
127     while (!p2.pointInBounds(pos) & counter < 100);
128     child.setSpatialPosition(pos);
129     return T;
130 }
131 150 late() { // last generation
132     allind1 = p1.individuals[p1.pointInBounds(p1.individuals.spatialPosition)];
133     allind2 = p2.individuals[p2.pointInBounds(p2.individuals.spatialPosition)];
134     sampledIndividuals = c(sample(allind1, nsam), sample(allind2, nsam));
135     sampledIndividuals.genomes.outputVCF(filePath="tmp.VCF", outputMultiallelics = F,
136         simplifyNucleotides=T);
137
138     out = paste("subpopulation", "pedigreeID", "x", "y", "genome1", "genome2");
139     for (i in sampledIndividuals){
140         info = paste(i.subpopulation, i.pedigreeID, i.spatialPosition, i.genome1.
141             nucleotides(), i.genome2.nucleotides());
142     }
143     out = c(out, info);
144     writeFile("coordgenomes.txt", out);
145 }

```

Listing 3: SLiM script for the *distinctness* scenario

```

1 species all initialize() {
2     defineConstant("L", 1e3);
3     defineConstant(symbol="nsim", value=200);
4     defineConstant(symbol="nsam", value=45);
5     defineConstant(symbol="i1sd", value=1);
6     defineConstant(symbol="i2maxd", value=3);
7     defineConstant(symbol="nneigh", value=3);
8     defineConstant(symbol="childsd", value=9);
9
10    // spatial competition
11    initializeInteractionType(1, "xy", reciprocal=T, maxDistance=3*i1sd);

```

```

12     i1.setInteractionFunction("n", i1sd/2, i1sd);
13
14     // spatial mate choice
15     initializeInteractionType(2, "xy", reciprocal=T, maxDistance=i2maxd);
16 }
17
18 species sunflower initialize() {
19     initializeSpecies(tickModulo=1, tickPhase=1, avatar="S");
20     initializeSLiMOptions(keepPedigrees = T, dimensionality="xy", nucleotideBased=T);
21     initializeAncestralNucleotides(randomNucleotides(L, c(1, 1, 1, 1)));
22     initializeMutationTypeNuc("m1", 0.5, "f", 0.0);
23     initializeGenomicElementType("g1", m1, 1.0, mmJukesCantor(2.5e-3));
24     initializeGenomicElement(g1, 0, L-1);
25     initializeRecombinationRate(rates = 1e-8);
26 }
27
28 species tulip initialize() {
29     initializeSpecies(tickModulo=1, tickPhase=1, avatar="T");
30     initializeSLiMOptions(keepPedigrees = T, dimensionality="xy", nucleotideBased=T);
31     initializeAncestralNucleotides(randomNucleotides(L, c(1, 1, 1, 1)));
32     initializeMutationTypeNuc("m2", 0.5, "f", 0.0);
33     initializeGenomicElementType("g2", m2, 1.0, mmJukesCantor(2.5e-3));
34     initializeGenomicElement(g2, 0, L-1);
35     initializeRecombinationRate(rates = 1e-8);
36 }
37
38 ticks all 1 early() {
39     sunflower.addSubpop("p1", nsim);
40     tulip.addSubpop("p2", nsim);
41     p1.setSpatialBounds(c(50.00, 50.00, 100.00, 100.00));
42     p2.setSpatialBounds(c(100.00, 100.00, 150.00, 150.00));
43     p1.individuals.setSpatialPosition(p1.pointUniform(nsim));
44     p2.individuals.setSpatialPosition(p2.pointUniform(nsim));
45 }
46
47 ticks all 1: late() {
48     i1.evaluate(p1);
49     inds = p1.individuals;
50     competition = i1.totalOfNeighborStrengths(inds) / size(inds);
51     competition = pmin(competition, 0.99);
52     inds.fitnessScaling = 1 - competition;
53
54     i1.evaluate(p2);
55     inds = p2.individuals;
56     competition = i1.totalOfNeighborStrengths(inds) / size(inds);
57     competition = pmin(competition, 0.99);
58     inds.fitnessScaling = 1 - competition;
59 }
60
61 ticks all 2: first() {
62     i2.evaluate(p1);
63     i2.evaluate(p2);
64 }
65
66 // NEAREST NEIGHBORS MATE CHOICE
67 species sunflower 2: mateChoice(p1) {
68     // nearest-neighbor mate choice
69     neighbors = i2.nearestNeighbors(individual, count = nneigh);
70     return (size(neighbors) ? sample(neighbors, 1) else float(0));
71 }

```

```

72 species tulip 2: mateChoice(p2) {
73     // nearest-neighbor mate choice
74     neighbors = i2.nearestNeighbors(individual, count = nneigh);
75     return (size(neighbors) ? sample(neighbors, 1) else float(0));
76 }
77 species sunflower modifyChild(p1) {
78     do pos = parent1.spatialPosition + rnorm(2, 0, childsd);
79     while (!p1.pointInBounds(pos));
80     child.setSpatialPosition(pos);
81
82     return T;
83 }
84 species tulip modifyChild(p2) {
85     do pos = parent1.spatialPosition + rnorm(2, 0, childsd);
86     while (!p2.pointInBounds(pos));
87     child.setSpatialPosition(pos);
88
89     return T;
90 }
91
92 ticks all 50 late() { // last generation
93     allind1 = p1.individuals;
94     allind2 = p2.individuals;
95     sampled1 = sample(allind1, nsam);
96     sampled2 = sample(allind2, nsam);
97     sampledIndividuals = c(sampled1, sampled2);
98
99     out = paste("subpopulation", "pedigreeID", "x", "y", "genome1", "genome2");
100    for (i in sampledIndividuals){
101        info = paste(i.subpopulation, i.pedigreeID, i.spatialPosition, i.genome1.
102        nucleotides(), i.genome2.nucleotides());
103        out = c(out, info);
104    }
105    writeFile("coordgenomes.txt", out);
}

```


C.2 GSpace

Script editing, software executions and data analysis were carried out in R. Variables like `Sequence_Size` or `Dispersal_Distribution` were modified according to the scenario at hand.

When only one software execution was involved (trivial conspecificity scenario), all individuals from the two groups were simulated at once, using a longer sequence of random coordinates next to the `Sample_Coordinate` variables. In all other situations, the code was run twice with a reduced number of coordinate pairs (e.g., six or four for the first group with equal-sized and unequal-sized groups, respectively), each time fulfilling the geographic separation explained in the main text: e.g., individuals from the first group would have coordinates bound within point (70,70) and point (90,90).

Listing 4: Common structure of the GSpace script

```
1  %%%%%%%%% SIMULATION SETTINGS %%%%%%%%%%
2  Setting_Filename = GSpaceSettings.txt
3  Random_seeds = 11000
4  Run_Number = 1
5
6  %%%%%%%%% OUTPUT FILE FORMAT SETTINGS %%%%%%%%%
7  Output_Dir = .
8  Data_File_Name = trial
9  Data_File_Extension = .txt
10
11  Genepop = True
12  Genepop_ind_file = F
13  Genepop_Group_All_Samples = T
14
15  Approximate_time = F
16
17  %%%%%%%%% MARKERS SETTINGS %%%%%%%%%%
18  Ploidy = Diploid
19  Chromosome_number = 1
20  Mutation_Rate = 0.005
21  Mutation_Model = KAM
22  Allelic_Lower_Bound = 240
23  Allelic_Upper_Bound = 241
24  Sequence_Size = 100
25
26  %%%%%%%%% RECOMBINATION SETTINGS %%%%%%%%%%
27  Recombination_Rate = 0.005
28
29  %%%%%%%%% DEMOGRAPHIC SETTINGS %%%%%%%%%%
30  %% LATTICE
31  Min_Sample_Coord_X = 50
32  Min_Sample_Coord_Y = 50
33  Lattice_Size_X = 200
34  Lattice_Size_Y = 200
35  Ind_Per_Node = 1
36
37  %% DISPERSAL
38  Dispersal_Distribution = p
39  Pareto_Shape = 5
40
41  Edge_Effects = circular
42  Total_Emigration_Rate = 0.5
43  Disp_Dist_Max = 200, 200
44
45  %%%%%%%%% SAMPLE SETTINGS %%%%%%%%%%
46  Sample_Coordinate_X = 82,84,70,82,75,71,115,127,130,122,128,124
```

```
47 Sample_Coordinate_Y = 89,76,89,72,73,70,111,116,128,120,117,129
48
49 % STATS
50 Dist_Class_Nbr = 1
51 Ind_Per_Node_Sampled = 1
52 Pause = Never
```